ISSN 2432-745X

Medical Mass Spectrometry

Vol. 9 No. 1, 2025
Guest Editor, Ikuko Yao

Preface
The 49th Annual Meeting of the Japanese Society for Biomedical Mass Spectrometry
..... Ikuko Yao, Makoto Arita, Toshimitsu Niwa 1

Mini Review
Picosecond Infrared Laser Mass Spectrometry for the Analysis of Biological Materials
..... Kenji Nakayama, Kazuo Igarashi, Arash Zarrine-Afsar 2

Research Papers
A case of N^5, N^{10}-methylenetetrahydrofolate reductase deficiency found by a pilot newborn screening for hypomethioninemia
..... Reiko Kagawa, Takako Maeda, Fumiaki Sakura, Miori Yuasa, Yosuke Shigematsu, Hideo Sasai, Masahisa Kobayashi, Takashi Hamazaki, Satoshi Okada, Go Tajima 8

Polyamine-based isolation of extracellular vesicles:
Examination in suspension cells and mechanistic considerations
..... Arizumi Kikuchi, Motoki Mori, Yuria Tachibana, Azumi Naruse, Kenichi Nonaka, Kimiaki Takagi, Keiko Kano, Emi Mishiro-Sato, Kaname Tsutsumiuchi 14

Short Communication
A case of primary meningococcal conjunctivitis in a young Japanese man rapidly identified as *Neisseria meningitidis* by MALDI-TOF MS
..... Noriko Mukai, Yukiya Takeichi, Yamato Yoshikawa, Kensuke Tajiri, Toyofumi Nakanishi, Teruyo Kida 23

Japanese Society for
Biomedical Mass Spectrometry

Medical Mass Spectrometry

Editorial Board

Published by Japanese Society for Biomedical Mass Spectrometry
Shubun University
6 Nikko-cho, Ichinomiya, Aichi 491−0938, Japan
E-mail: jsbms.office@gmail.com
Homepage: http://www.jsbms.jp/english/

Preface

The 49th Annual Meeting of the Japanese Society for Biomedical Mass Spectrometry

Ikuko Yao[1]*, Makoto Arita[2,3,4], Toshimitsu Niwa[5]

The 49th Annual Meeting of the Japanese Society for Biomedical Mass Spectrometry (JSBMS) in conjunction with the 3rd International Symposium of JSBMS and Mass Spectrometry and Advances in the Clinical Lab (MSACL) was held on September 13th and 14th, 2024, at Shimadzu Corporation, Kyoto, Japan. We were fortunate to gather in person and engage in lively scientific discussions across a wide range of topics.

The program included an award lecture, three symposia featuring 11 presentations, and two luncheon seminars. A total of 69 abstracts were submitted, of which 16 were selected for oral presentations. In addition, 60 abstracts were presented as posters, contributing to vibrant and productive exchanges among participants.

This 9th issue of Medical Mass Spectrometry is based on the presentations delivered at the 49th Annual Meeting of JSBMS and the 3rd International Symposium of JSBMS and MSACL in Kyoto. One of the highlights was the invited lecture by Dr. Arash Zarrine-Afsar from the University of Toronto, in which he presented his pioneering work on rapid pathological diagnostics. A detailed account of his innovative approach is included in this issue.

The 50th Annual Meeting of JSBMS will be held on September 12th and 13th, 2025, under the organization of Professor Tomoko Oya. We look forward to welcoming you to Ichinomiya, Aichi, and continuing our shared pursuit of advancements in medical mass spectrometry.

[1]School of Biological and Environmental Sciences, Kwansei Gakuin University
*E-mail: yaoik@kwansei.ac.jp
[2]Division of Physiological Chemistry and Metabolism, Keio University Faculty of Pharmacy
[3]Laboratory for Metabolomics, RIKEN Center for Integrated Medical Sciences
[4]Cellular and Molecular Epigenetics Laboratory, Graduate School of Medical Life Science, Yokohama City University
[5]Shubun University
Epub June 9, 2025.
DOI: 10.24508/mms.2025.06.005

Mini Review

Picosecond Infrared Laser Mass Spectrometry for the Analysis of Biological Materials

Kenji Nakayama[1, 2*], Kazuo Igarashi[3], Arash Zarrine-Afsar[4, 5, 6, 7]

[1]Research Center for BioMedical Analysis, Niigata University of Health and Welfare, Niigata 950−3198, Japan
[2]Department of Urology, Kyoto University Hospital, 54 Shogoin-kawahara-cho, Sakyo-ku, Kyoto 606−8507, Japan
[3]Association for Medicinal Analysis, Koyochonaka, Higashinada-ku, Kobe 658−0032, Japan
[4]Princess Margaret Cancer Centre, University Health Network, Toronto, ON, M5G 1L7, Canada
[5]Department of Medical Biophysics, University of Toronto, Toronto, ON, M5G 1L7, Canada
[6]Department of Surgery, University of Toronto, Toronto, ON, M5T 1P5, Canada
[7]Keenan Research Center for Biomedical Science & the Li Ka Shing Knowledge Institute, St. Michael's Hospital, Toronto, ON, M5B 1W8, Canada

Abstract The 49th Annual Meeting of the Japanese Society for Biomedical Mass Spectrometry (JSBMS) featured the 3rd International Joint Symposium with Mass Spectrometry: Applications to the Clinical Lab (MSACL), marking the first in-person collaboration. Dr. Arash Zarrine-Afsar, Department of Medical Biophysics, University of Toronto, presented "10-Second Cancer Diagnosis with Picosecond Infrared Laser Mass Spectrometry (PIRL-MS)," highlighting PIRL-MS technology. This method combines two innovations: PIRL-DIVE (**p**icosecond **i**nfrared **l**aser ablation/**d**esorption by **i**mpulsive **v**ibrational **e**xcitation) for precise biomolecule extraction and ion detection without conventional sources for minimally invasive diagnostics. The PIRL-MS enables intact biomolecule analysis, tissue classification, and cancer biomarker detection with minimal tissue damage. These advancements make the PIRL-MS a promising intraoperative diagnostics and biomedical research tool. This mini-review focuses on the evolution of his method and briefly summarizes the discoveries and applications that led to this method.

Key words: picosecond infrared laser (PIRL), mass spectrometry (MS), picosecond infrared laser ablation/desorption by impulsive vibrational excitation (PIRL-DIVE)

Abbreviations: PIRL, picosecond infrared laser; DIVE, desorption by impulsive vibrational excitation; PIRL(A), picosecond infrared laser ablation; MS, mass spectrometry

Introduction

The 49th Annual Meeting of the Japanese Society for Biomedical Mass Spectrometry (JSBMS) was held at the Shimadzu Corporation Hall in Kyoto on September 13−14, 2024. As part of this event, the 3rd International Joint Symposium of the JSBMS and Mass Spectrometry: Applications to the Clinical Lab (MSACL) was convened. This symposium represented the first opportunity for an in-person international joint symposium, as the first and second editions were conducted online due to the global COVID-19 pandemic. On this occasion, MSACL nominated Dr. Arash Zarrine-Afsar as their representative speaker, and the JSBMS International Committee invited him to participate. Dr. Zarrine-Afsar delivered an outstanding presentation entitled "10-Second Cancer Diagnosis with Picosecond Infrared Laser Mass Spectrometry[1)]."

* **Corresponding author**
Kenji Nakayama
Research Center for BioMedical Analysis, Niigata University of Health and Welfare, Room F105, 1398 Shimami-cho, Kita-ku, Niigata-shi, Niigata 950−3198, Japan
Tel: +81−25−257−4746, Fax: +81−25−257−4456
E-mail: kenji-nakayama@nuhw.ac.jp
Received: January 23, 2025. Accepted: April 10, 2025.
Epub May 22, 2025.
DOI: 10.24508/mms.2025.06.002

Dr. Zarrine-Afsar presented his work on intraoperative molecular diagnosis using picosecond infrared laser mass spectrometry (PIRL-MS)[2], a novel application of mass spectrometry that in a manner similar to rapid evaporative ionization mass spectrometry (REIMS)[3] has shown potential in biomedical research. REIMS, along with other ambient mass spectrometry analysis methods, represents a significant advancement in clinical mass spectrometry by enabling real-time, direct analysis of biological tissues without the need for complex sample preparation or chromatographic separation. This approach is particularly valuable in clinical settings where rapid and accurate results are essential. By analyzing the molecular composition of surgical aerosols, REIMS facilitates rapid tissue classification, disease detection, and intraoperative diagnostics[2–4]. Furthermore, its integration with machine learning algorithms enhances diagnostic accuracy and tissue classification. As clinical mass spectrometry advances toward point-of-care applications, REIMS demonstrates remarkable potential by bridging the gap between laboratory analysis and real-time clinical decision-making[2–5].

Following his presentation, the symposium organizers acknowledged the significance of his methodology and expressed their intention to explore and introduce his innovative technique in this journal. With his kind cooperation, this initiative aims to enhance the understanding of Japanese medical mass spectrometrists and promote the adoption of this advanced approach in clinical practice.

This mini-review, prepared with the kind cooperation of Dr. Zarrine-Afsar, aims to introduce his picosecond infrared laser mass spectrometry (PIRL-MS) to the members of JSBMS. The mini-review is structured into three sections: (1) the initial discovery of PIRL(A)-DIVE (**p**icosecond **i**nfrared **l**aser **a**blation/**d**esorption by **i**mpulsive **v**ibrational **e**xcitation), (2) the attractive integration of PIRL(A) technology with electrospray ionization (ESI), and (3) the breakthrough detection of ionized biomolecules without conventional ion sources. For clarity and accessibility, this mini-review adopts the term "PIRL(A)" instead of the original PIRL, with kind permission from Dr. Zarrine-Afsar.

1. The Initial Discovery of PIRL(A)-DIVE (Picosecond Infrared Laser Ablation/Desorption by Impulsive Vibrational Excitation) Phenomenon

Picosecond infrared laser (PIRL) technology was developed and proposed to overcome the limitations of conventional medical lasers in achieving single-cell precision cutting, essential for minimally invasive procedures and tissue restructuring by Dr. R. J. Dwayne Miller[6, 7]. Traditional lasers failed to reach this precision due to collateral damage caused by thermal and shock wave effects on surrounding tissue. The PIRL ablation offered a groundbreaking solution by selectively energizing water molecules in the tissue much faster than heat transfer from superheated water molecules to their surroundings[8–10]. This process drove ablation or cutting faster than thermal energy could spread, thus avoiding the collateral damage inherent in other laser technologies[7–11]. Unlike conventional lasers, PIRL did not produce plasma formation or harmful ionizing radiation effects[7, 9–11]. The advantage of PIRL technology lies in its minimal energy deposition in the surrounding tissue, eliminating photochemical and photothermal side effects. This precision-made PIRL uniquely suited for delicate medical applications, representing a significant advancement in laser-based surgical techniques[7, 9, 11, 12].

In 2015, Ren et al., from Dr. Miller's group, introduced an innovative method known as PIRL ablation, based on the desorption by impulsive vibrational excitation (DIVE) principle[13]. This technique enabled the efficient extraction of biological entities from aqueous and natural environments into aerosols (Fig. 1), preserving their biological integrity and activity. Key findings were demonstrated that extracted enzymes retained enzymatic activity without oxidation, denaturation, or inactivation; metabolic molecules remained intact without oxidation or fragmentation; nucleic acids, including DNAs and RNAs, were retrieved in their native forms; and infectious viruses were recovered with preserved infectivity. In addition, of particular interest, the rapid extraction of proteins has promised novelties in future use for proteomic applications[14]. Unlike conventional methods that often involve harsh chemicals or heat, the DIVE-driven PIRL (hereafter referred to as PIRL(A)-DIVE) method precisely targeted water molecules, minimizing thermal and mechanical stress. This ensured the structural and functional preservation of biological materials, establishing the PIRL(A)-DIVE as a valuable tool for sensitive biological extractions in research and medical applications. Not limited to its potential as an instantaneous tool with micrometer precision for biopsy, the PIRL(A)-DIVE method brought promising benefits to chemical analysis, biological diagnosis, and disease control[13, 15]. Further-

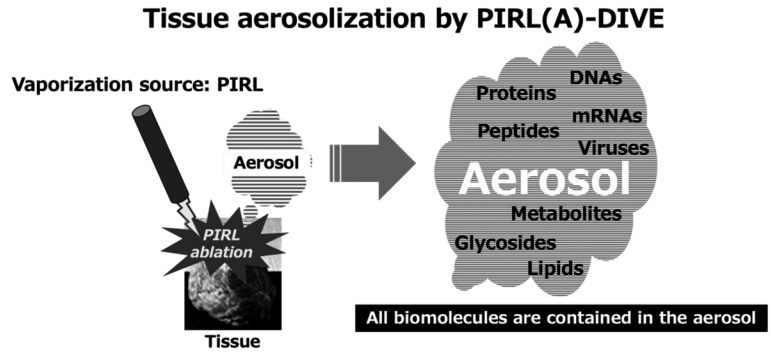

Fig. 1. The initial discovery of PIRL(A)-DIVE (Picosecond Infrared Laser Ablation/Desorption by Impulsive Vibrational Excitation) phenomenon.

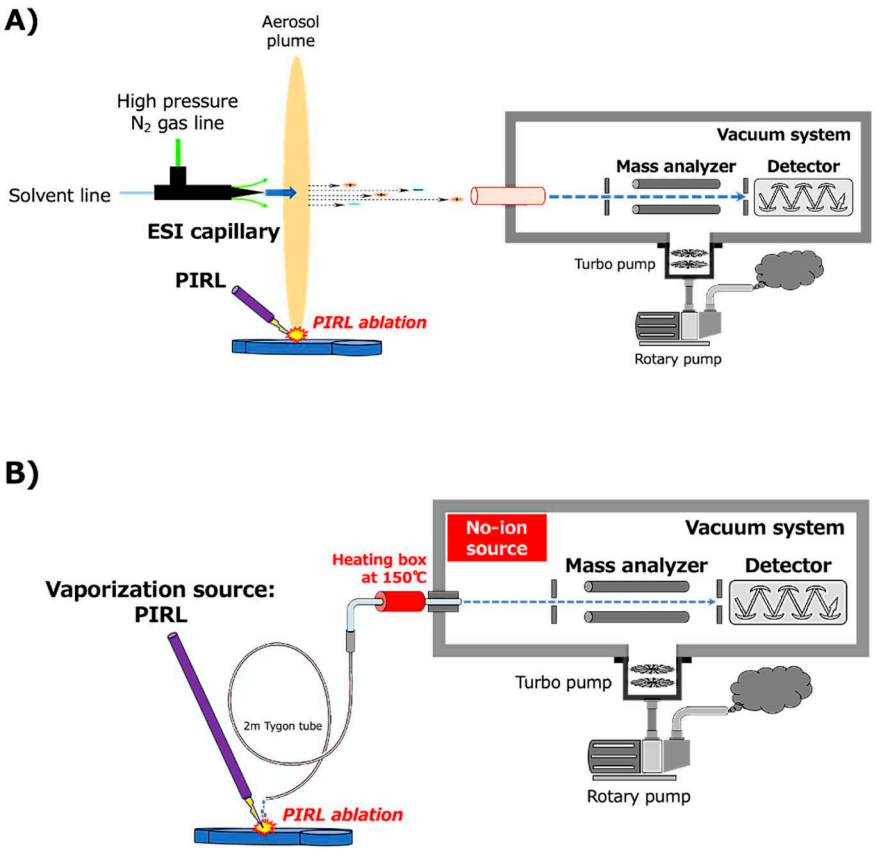

Fig. 2. Analytical technologies of PIRL(A)-MS combining two groundbreaking discoveries.
A) The attractive integration of the PIRL(A)-DIVE and electrospray ionization (ESI) technologies. B) The breakthrough detection of ionized biomolecules through the heating box at 150°C without conventional ion sources.

more, applications of PIRL(A)-DIVE conducted under atmospheric conditions, demonstrated its exceptional effectiveness in extracting molecules from water-rich biological materials and its suitability for characterizing biological tissues with high water content. Subsequent studies utilizing PIRL(A)-DIVE have revealed that the technique induces minimal tissue damage beyond the ablation zone, emphasizing its significant potential for a wide range of biomedical applications[2, 13].

2. The Attractive Integration of the PIRL(A)-DIVE and Electrospray Ionization (ESI) Technologies

In 2015, the attractive integration of the PIRL(A)-DIVE and ESI technologies was attempted and reported by Dr. Arash Zarrine-Afsar's group in collaboration with Dr. R. J.

Dwayne Miller[16]. As shown in Fig. 2, both PIRL(A)-DIVE and ESI were integrated to develop a novel analytical system for imaging mass spectrometry, which has been successfully reported[16]. PIRL(A) was employed to generate a plume directly from the target bio-material. This plume contained all intact biomolecules, preserved in an aerosol-like state. The plume was subsequently intercepted by an electrospray, which efficiently ionized the biomolecules. The resulting ions were then transferred to a mass spectrometry (MS) detector for analysis. This process enabled the direct and gentle ionization of biomolecules, preserving their structural integrity. This PIRL(A)-ESI-MS system was utilized to image the distribution of gadoteridol, an exogenous magnetic resonance contrast agent that was administered via intravenous injection into the tail vein of the mice, within mouse kidneys[16]. This study also demonstrated that PIRL(A)-ESI is capable of performing desorption ionization of small molecules, proteins as well as phospholipids[16] and concluded that PIRL(A)-ESI is a suitable ion source for potential future applications in ambient mass spectrometry. Notably, a PIRL probe combined with secondary ionization techniques, such as ESI, and mass spectrometry holds significant potential for providing molecular feedback to guide laser surgery. Since this initial implementation, additional studies utilizing PIRL(A)-DIVE have suggested that the technique induces minimal tissue damage outside the ablation zone, highlighting its promise for further biomedical applications[2, 16].

3. The Breakthrough Detection of Ionized Biomolecules without Conventional Ion Sources

In 2017, Woolman et al., from Dr. Zarrine-Afsar's group, utilized the efficient and rapid extraction capabilities of PIRL, combined with the plume's rapid cooling upon expansion, to investigate the potential of coupling PIRL(A) with soft ionization techniques like thermal desolvation[17]. This innovative approach enabled the analysis of pre-charged lipid molecules carrying negative charges, leading to the development of a novel analytical platform termed PIRL-MS which is referred to herein as PIRL(A)-MS to highlight the ablative mechanism behind the laser action. Notably, this discovery and implementation were built on the previous creation of PIRL desorption, and only added a suitable means of ionization, as illustrated in Fig. 2B. Woolman et al. demonstrated that negatively charged lipids could be detected in an MS system without using an external ion source per se such as ESI, requiring only biomolecule heating at 150°C before introducing into the MS device to prevent resolvation[17]. Furthermore, this method successfully classified mouse organs based on extracted and desolvated lipid molecules analyzed in the negative ion mode. An international patent subsequently protected this groundbreaking technology[18].

Independent subcutaneous murine xenograft tumors—derived from six distinct, well-established human medulloblastoma cell lines representing the Sonic Hedgehog and Group 3 subgroups—were analyzed using the PIRL(A)-MS system[19, 20]. Following the efficient classification of mouse organs, tumor analytical data were further evaluated through multivariate statistical analysis, with robustness validated via an iterative 5%-leave-out-and-remodel approach. Additionally, the potential of integrating PIRL(A)-MS with imaging modalities, such as wide-field tissue polarimetry for cancer region guidance, was explored. Polarimetric imaging was used to identify tissue heterogeneities, effectively directing the PIRL desorption source. The PIRL(A)-MS plume was transported to the mass spectrometer through a 2-meter-long Tygon tube, facilitating the development of a handheld MS point sampling device for analyzing thick tissue sections *in situ*[2, 17]. Specifically, PIRL(A)-MS point sampling, guided by polarimetry, successfully identified necrotic regions in metastatic breast tumors and efficiently detected the necrotic cancer marker ion at *m/z* 572.48 ([ceramide (d34:1)+Cl]$^-$)[2, 17]. Polarimetry-directed sampling precisely targeted necrotic areas, while PIRL(A)-MS spectra revealed the presence of common fatty acids and phospholipids, consistent with findings from other MS techniques used for breast cancer analysis. These results underscored the potential of combining polarimetric imaging with PIRL(A)-MS for accurate and targeted tissue analysis in complex biological samples. Subsequently, the hand-held PIRL(A)-MS probe has been used in several patient specimen explorations to determine various tumor pathologies faster than currently possible. These have included rapid exploratory subgrouping of human medulloblastoma[20] and other pediatric brain cancer types[21], human skin cancer[22] and 10-second identification of actionable BRAF-V600E mutation[23]. Integration of PIRL(A)-MS probe with surgical positioning and navigation technologies has enabled on-the-spot delivery of MS-based pathology classifications via virtual reality augmentation[24].

This mini-review considered a potential mechanism to explain why PIRL(A)-MS can detect negatively ionized lipid molecules. The two hypotheses were offered: (1) the detectable ionization may occur solely through the application of heat, depending on the specific type of biomolecule, and (2) a proportion of molecules in living organisms naturally exist in a negatively charged state such as anionic phospholipids[25, 26], which the PIRL(A)-MS system can effectively detect and analyze as in vivo ionized biomolecules, especially anionic phospholipids.

Conclusions

The PIRL(A)-MS is a technology that has advanced significantly through the successful integration of two groundbreaking discoveries, as mentioned earlier, and has emerged as a highly promising analytical tool. The keynote lecture titled "10-Second Cancer Diagnosis with Picosecond Infrared Laser Mass Spectrometry[1]" presented a revolutionary and pioneering research topic that leveraged these technological advancements to develop a novel intraoperative molecular diagnostic method. In Japan, the medical application of mass spectrometry has not yet advanced to the level of intraoperative molecular diagnosis. Therefore, the active contributions of young JSBMS members are eagerly anticipated to drive future progress in this field.

Declaration of Competing Interest

AZA is an inventor of the soft ionization method for PIRL-MS and is a consultant with Point Surgical Inc. with a financial interest.

Acknowledgements

We would like to express our deepest gratitude to Dr. Ikuko Yao, Chair of the 49th Annual Meeting of the JSBMS, and Dr. Toshimitsu Niwa, President of the JSBMS, for presenting us with this wonderful opportunity. Additionally, we extend our sincere thanks to Dr. David Herold, President of MSACL, and Dr. Michael Chen, Co-Chair of the Asia Outreach Committee of MSACL, for their generous support and guidance. We express our deepest gratitude to JEOL Ltd. for permitting us to use and modify their original illustration of a mass spectrometer as part of this work. Their generous support and cooperation have greatly contributed to the quality and clarity of this mini-review. We sincerely appreciate their understanding and collaboration.

References

1) Zarrine-Afsar A: 10-second cancer diagnosis with picosecond infrared laser mass spectrometry (PIRL-MS). *JSBMS Lett* 49 (Supplement): 38, 2024.
2) Tata A, Woolman M, Bluemke E, Zarrine-Afsar, A: Chapter 5—Ambient laser-based mass spectrometry analysis methods: A survey of core technologies and reported applications, in Zaitsu K (eds): *Ambient ionization mass spectrometry in life sciences*. pp. 119−169, Elsevier, Amsterdam, 2020.
3) Balog J, Sasi-Szabo L, Kinross J, Lewis MR, Muirhead LJ, et al: Intraoperative tissue identification using rapid evaporative ionization mass spectrometry. *Sci Transl Med* 5: 194ra93, 2013.
4) Ogrinc N, Saudemont P, Takats Z, Salzet M, Fournier I: Cancer Surgery 2.0: Guidance by real-time molecular technologies. *Trends Mol Med* 27: 602−615, 2021.
5) Zhang J, Sans M, Garza KY, Eberlin LS: Mass spectrometry technologies to advance care for cancer patients in clinical and intraoperative use. *Mass Spectrom Rev* 40: 692−720, 2020.
6) Girard B, Yu D, Armstrong MR, Wilson BC, Clokie CM, et al: Effects of femtosecond laser irradiation on osseous tissues. *Lasers Surg Med* 39: 273−285, 2007.
7) Amini-Nik S, Kraemer D, Cowan ML, Gunaratne K, Nadesan P, et al: Ultrafast mid-IR laser scalpel: Protein signals of the fundamental limits to minimally invasive surgery. *PLoS One* 5: e13053, 2010.
8) Cowan ML, Bruner BD, Huse N, Dwyer JR, Chugh B, et al: Ultrafast memory loss and energy redistribution in the hydrogen bond network of liquid H_2O. *Nature* 434: 199−202, 2005.
9) Franjic K, Cowan ML, Kraemer D, Miller RJ: Laser selective cutting of biological tissues by impulsive heat deposition through ultrafast vibrational excitations. *Opti Express* 17: 22937−22959, 2009.
10) Franjic K, Miller D: Vibrationally excited ultrafast thermodynamic phase transitions at the water/air interface. *Phys Chem Chem Phys* 12: 5225−5239, 2010.
11) Hess M, Hildebrandt MD, Müller F, Kruber S, Kroetz P, et al: Picosecond infrared laser (PIRL): An ideal phonomicrosurgical laser? *Eur Arch Otorhinolaryngol* 270: 2927−2937, 2013.
12) Mehlan J, Uschold S, Hansen NO, Gosau T, Eggert D, et al: Picosecond infrared laser fiber-assisted sclerostomy (PIRL-FAST): A first proof of principle analysis. *Ophthal-*

mologe 116: 346−350, 2019.

13) Ren L, Robertson WD, Reimer R, Heinze C, Schneider C, et al: Towards instantaneous cellular level bio diagnosis: Laser extraction and imaging of biological entities with conserved integrity and activity. *Nanotechnology* 26: 284001, 2015.
14) Kwiatkowski M, Wurlitzer M, Omidi M, Ren L, Kruber S, et al: Ultrafast extraction of proteins from tissues using desorption by impulsive vibrational excitation. *Angew Chem Int Ed Engl* 54: 285−288, 2015.
15) Gottardi R: Towards a minimally invasive sampling tool for high resolution tissue analytical mapping. *Nanotechnology* 26: 372501, 2015.
16) Zou J, Talbot F, Tata A, Ermini L, Franjic K, et al: Ambient mass spectrometry imaging with picosecond infrared laser ablation electrospray ionization (PIR-LAESI). *Anal Chem* 87: 12071−12079, 2015.
17) Woolman M, Gribble A, Bluemke E, Zou J, Ventura M, et al: Optimized mass spectrometry analysis workflow with polarimetric guidance for ex vivo and in situ sampling of biological tissues. *Sci Rep* 7: 468, 2017.
18) Zarrine-Afsar A, Ginsberg HJ, Woolman M: Soft ionization system and method of use thereof. WO2017214718A3. 2017.12.21.
19) Woolman M, Ferry I, Kuzan-Fischer CM, Wu M, Zou J, et al: Rapid determination of medulloblastoma subgroup affiliation with mass spectrometry using a handheld picosecond infrared laser desorption probe. *Chem Sci* 8: 6508−6519, 2017.
20) Woolman M, Kuzan-Fischer CM, Ferry I, Kiyota T, Luu B, et al: Picosecond infrared laser desorption mass spectrometry identifies medulloblastoma subgroups on intra-surgical timescales. *Cancer Res* 79: 2426−2434, 2019.
21) Woolman M, Kiyota T, Belgadi SA, Fujita N, Fiorante A, et al: Lipidomic-based approach to 10 s classification of major pediatric brain cancer types with picosecond infrared laser mass spectrometry. *Anal Chem* 96: 1019−1028, 2024.
22) Katz L, Woolman M, Kiyota T, Pires L, Zaidi M, et al: Picosecond infrared laser mass spectrometry identifies a metabolite array for 10 s diagnosis of select skin cancer types: A proof-of-concept feasibility study. *Anal Chem* 94: 16821−16830, 2022.
23) Katz L, Kiyota T, Woolman M, Wu M, Pires L, et al: Metabolic lipids in melanoma enable rapid determination of actionable BRAF-V600E mutation with picosecond infrared laser mass spectrometry in 10 s. *Anal Chem* 95: 14430−14439, 2023.
24) Woolman M, Qiu J, Kuzan-Fischer CM, Ferry I, Dara D, et al: *In situ* tissue pathology from spatially encoded mass spectrometry classifiers visualized in real time through augmented reality. *Chem Sci* 11: 8723−8735, 2020.
25) Dowhan W: Molecular basis for membrane phospholipid diversity: Why are there so many lipids? *Annu Rev Biochem* 66: 199−232, 1997.
26) Dubois GA, Jaillais Y: Anionic phospholipid gradients: An uncharacterized frontier of the plant endomembrane network. *Plant Physiol* 185: 577−592, 2021.

Research Paper

A case of N^5, N^{10}-methylenetetrahydrofolate reductase deficiency found by a pilot newborn screening for hypomethioninemia

Reiko Kagawa[1], Takako Maeda[2], Fumiaki Sakura[1], Miori Yuasa[3], Yosuke Shigematsu[3], Hideo Sasai[4], Masahisa Kobayashi[5], Takashi Hamazaki[6], Satoshi Okada[1], Go Tajima[1,2]*

[1]Department of Pediatrics, Hiroshima University Graduate School of Biomedical and Health Sciences, 1−2−3 Kasumi, Minami-ku, Hiroshima 734−8551, Japan
[2]Division of Neonatal Screening, Research Institute, National Center for Child Health and Development, 2−10−1 Okura, Setagaya-ku, Tokyo 157−8535, Japan
[3]Department of Pediatrics, School of Medical Sciences, University of Fukui, 23−3 Matsuoka-Shimoaizuki, Eiheiji-cho, Fukui 910−1193, Japan
[4]Department of Early Diagnosis and Preventive Medicine for Rare Intractable Pediatric Diseases, Graduate School of Medicine, Gifu University, 1−1 Yanado, Gifu 501−1119, Japan
[5]Department of Pediatrics, The Jikei University School of Medicine, 3−25−8 Nishishinbashi, Minato-ku, Tokyo 105−8461, Japan
[6]Department of Pediatrics, Osaka Metropolitan University Graduate School of Medicine, 1−4−3 Asahimachi, Abeno-ku, Osaka 545−8585, Japan

Abstract Current newborn screening (NBS) in Japan detects homocystinuria type 1 by elevated levels of methionine (Met), which is insufficient to detect homocystinuria types 2 and 3 that are associated with hypomethioninemia. We have conducted a pilot NBS for inborn errors of cobalamin metabolism in Hiroshima area of Japan since 2018, using the ratio of propionylcarnitine (C3) to Met (C3/Met) and low Met level as markers. We found a newborn female with low Met (9.54 μmol/L, cutoff ＜10 μmol/L) without elevated C3 or C3/Met in a dried blood specimen collected 4 days post-birth. Second-tier tests revealed slightly elevated total homocysteine (tHcy) (15.7 μmol/L, cutoff ≥5.0 μmol/L) but normal methylmalonic acid (MMA) levels. At 20 days of age, plasma tHcy rose to 52.0 μmol/L, with slightly elevated MMA (3.9 μmol/L, cutoff ≥1.0 μmol/L) and decreased serum vitamin B_{12} (VB_{12}: 146 pg/mL, reference range 197−771 pg/mL). Gene panel analysis of related disorders detected two *MTHFR* variants: p.G149V (c. 447delinsTT) and p.P65L (c.193T＞C). 5,10-methylenetetrahydrofolate reductase (MTHFR) activity in lymphocytes and in a dried blood specimen were 56.27 μU/mg protein (8.40% of mean control value) and 50.19 mmol/min/L (11.5% of mean control value), respectively. On the basis of a diagnosis of MTHFR deficiency associated with mild VB_{12} deficiency, we initiated betaine and mecobalamin administration. The successful detection of this mild case of MTHFR deficiency suggests a good sensitivity of our pilot NBS for the disease, while the combination of second-tier tHcy and MMA measurements is required to retain an appropriate level of specificity.

Key words: disorders of cobalamin metabolism, homocystinuria, hypomethioninemia, methylmalonic acidemia, newborn screening

*Corresponding author
Go Tajima
Division of Neonatal Screening, Research Institute, National Center for Child Health and Development, 2−10−1 Okura, Setagaya-ku, Tokyo 157−8535, Japan
Tel: +81−3−5494−7133
E-mail: tajima-g@ncchd.go.jp
Received: January 10, 2025. Accepted: May 21, 2025.
Epub June 16, 2025.
DOI: 10.24508/mms.2025.06.003

Introduction

Current newborn screening (NBS) in Japan identifies methylmalonic acidemia and propionic acidemia by elevated levels of propionylcarnitine (C3), and homocystinuria (HCU) type 1 caused by cystathionine β-synthase (CBS) deficiency through elevated levels of methionine (Met) in dried blood specimens. However, C3 measurement is not always sufficiently sensitive to detect methylmalonic acidemia caused by defects in the pathway of adenosylcobalamin

synthesis. In HCU type 2 caused by defects in methylcobalamin synthesis and HCU type 3 caused by 5,10-methylenetetrahydrofolate reductase (MTHFR) deficiency, Met levels decrease due to disturbed remethylation of homocysteine. Because the prognosis of these diseases can be greatly improved by starting specific medication as soon as possible after birth[1–5], we have been conducting a pilot NBS for inborn errors of cobalamin metabolism in Hiroshima area of Japan since 2018, using C3/Met and low Met levels as first-tier markers, and total homocysteine (tHcy) and methylmalonic acid (MMA) as second-tier markers. In this report, we present our successful identification of an asymptomatic newborn with MTHFR deficiency.

Materials and Methods

Research subjects

Newborns from 10 major hospitals in Hiroshima area were enrolled into the pilot newborn screening (NBS) program following the provision of written informed consent for study participation from their parents. Dried blood specimens (DBS) for NBS were collected on the four or five days of old and analyzed at Hiroshima City Medical Association Clinical Laboratory.

Screening tests

First-tier screening tests used the following indices: index 1, C3 ≥3.6 μmol/L and C3/acetylcarnitine (C2) ≥0.23 (current NBS indices); index 2, C3/Met ≥0.25; and index 3, Met <10 μmol/L. Samples that met one or more of the three indices were transported to the National Center for Child Health and Development for the second-tier measurement of MMA (cutoff ≥1.0 μmol/L) and tHcy (cutoff ≥5.0 μmol/L). Newborns with elevated MMA and/or tHcy levels were further examined in the Department of Pediatrics, Hiroshima University Hospital.

Biochemical and genetic analysis

The analysis of amino acids and acylcarnitines in DBS was performed using an LCMS-8045 tandem mass spectrometer (Shimadzu, Kyoto, Japan) according to a previously described flow injection method[6] with some modification. The second-tier measurement of MMA and tHcy in DBS was performed using liquid chromatography–mass spectrometry (LCMS-8050, Shimadzu) according to previously described methods[7]. To confirm the diagnosis, panel analysis of genes engaged in cobalamin metabolism (*ABCD4*, *HCFC1*, *LMBRD1*, *MMAA*, *MMAB*, *MMACHC*, *MMADHC*, *MTR*, *MTRR*, *MTHFR*), methylmalonyl-CoA mutase (*MUT*) and propionyl-CoA carboxylase (*PCCA*, *PCCB*) was performed using next-generation sequencing with the MiSeq Sequencing System (Illumina, San Diego, CA, USA) at Kazusa DNA Research Institute (Chiba, Japan).

Results

Overall findings of the pilot NBS

Between April 2019 and September 2024, 21,105 out of a total of 103,602 newborns born in Hiroshima area were enrolled in the pilot NBS. The total number of cases positive for the first-tier tests was 267 (1.27%): 14 (0.06%) for index 1, 21 (0.10%) for index 2, and 232 (1.10%) for index 3. Some of these subjects were positive for two of the three indices: 6 (0.03%) for indices 1 and 2, and 24 (0.11%) for indices 2 and 3 (Table 1). In the second-tier tests, MMA was elevated in five cases, and tHcy was elevated in one case. These six cases were examined at Hiroshima University Hospital (Table 2). A diagnosis of methylmalonyl-CoA mutase deficiency was confirmed in two (cases 3 and 4), and that of MTHFR deficiency in one (case 6). Diagnoses for the other three (cases 1, 2, and 5) were not revealed by the gene panel analysis.

To evaluate whether positive rates for the three indices increased among low-birth-weight infants, we compared distribution of the values in DBS of infants with a birth weight <2,000 g with that of mature infants born between

Table 1. Overall results of the pilot screening from April 2019 to September 2024

	All newborns in Hiroshima area N=103,602	Newborns enrolled in this study N=21,105
C3 ≥3.6 μmol/L & C3/C2 ≥0.23 [+C3/Met ≥0.25]	302 (0.29%) [16]	14 (0.06%) [6]
C3/Met ≥0.25*	96 (0.09%)	21 (0.10%)
Met <10 μmol/L [+C3/Met ≥0.25]	530 (0.51%) [34]	232 (1.10%) [24]
Total	928 (0.90%)	267 (1.27%)
MMA ≥1.0 μmol/L	—	5
tHcy ≥5.0 μmol/L	—	1

*Number (rate) of C3/Met-positive cases without elevation of C3, C3/C2 or decrease of Met.

Table 2. Positive findings in the second-tier tests and the diagnoses

	C3 & C3/C2	Met	C3/Met	MMA	tHcy	Diagnosis
Cutoff	≥3.6 & ≥0.23	<10.0	≥0.25	≥1.0	≥5.0	
Case 1	2.87/0.14	7.89	0.36	1.2	1.0	VUS: compound heterozygous variant of *PCCA*
Case 2	4.46/0.23	22.79	0.20	1.0	4.8	VUS: compound heterozygous variant of *PCCA*（Siblings also showed a mild increase in MMA.）
Case 3	11.14/0.71	33.03	0.34	337.7	2.8	MUT deficiency
Case 4	11.26/0.64	15.27	0.74	559.5	2.9	MUT deficiency
Case 5	3.94/0.23	20.96	0.04	1.0	2.4	VUS: homozygous variant of *LMBRD1*
Case 6	1.39/0.08	9.54	0.14	<1.0	15.7	MTHFR deficiency

Table 3. Correlation between low birth weight and positive findings in the first-tier tests, methionine, phenylalanine and Met/Phe levels

	Birth Weight ≥2,000 g	Birth Weight <2,000 g	P
n (%)	18,080 (97.9%)	385 (2.1%)	—
Birth Weight (g)	3,026±237	1,670±86.5	<0.001
C3≥3.6 μmol/L& C3/C2 ≥0.23 [+C3/Met ≥0.25] n (%)	13 (0.07%) [4]	0	—
C3/Met ≥0.25 n (%)	13 (0.07%)	2 (0.52%)	<0.001
Met <10 μmol/L [+C3/Met ≥0.25] n (%)	32 (0.17%) [2]	37 (9.61%)	<0.001
Met (μmol/L)	21.66±0.85	16.83±9.25	<0.001
Phe (μmol/L)	44.76±10.94	46.23±9.54	<0.001
Met/Phe	0.48±0.11	0.36±0.08	<0.001

No association with low birth weight was found for index 1 (C3 ↑ & C3/C2 ↑), but the frequency of low birth weight infants increased for indices 2 (C3/Met ↑) and 3 (Met ↓). There was a tendency for low methionine levels in infants with a birth weight <2,000 g. Phenylalanine levels were higher for the low birth weight infants.

April 2022 and September 2023. We also compared levels of phenylalanine (Phe) between the two groups, because Met/Phe ratio could reportedly be a better marker for the diseases showing hypomethioninemia[4,8,9]. As a result, positive rates were higher in the low-birth-weight infants than in the mature infants for index 2 (0.52% versus 0.07%) and index 3 (9.61% versus 0.17%), while there was no significant difference for index 1. Distribution of Met levels was significantly lower in the low-birth-weight infants than in the mature infants (16.83±9.25 versus 21.66±0.85, mean±SD), while distribution of Phe levels was higher in the low-birth-weight infants than in the mature infants (46.23±9.54 versus 44.76±10.94, mean±SD) (Table 3).

Case Report

A baby girl (Case 6 shown in Table 2) born as the third child of healthy nonconsanguineous parents at 39 weeks' gestation with a birth weight of 2,420 g showed low Met level (9.54 μmol/L) in the pilot NBS test. Second-tier tests revealed slightly elevated tHcy level (15.7 μmol/L) but normal MMA level. At the first examination on the 20th day after birth, she was healthy and had been mostly breastfed. Her levels of plasma tHcy and serum MMA were elevated (52.0 μmol/L, cutoff ≥ 10.0 μmol/L; 3.9 μmol/L, cutoff ≥1.0 μmol/L, respectively) (Table 4). Because her serum vitamin B_{12} (VB_{12}) level was slightly low (146 pg/mL; reference range, 197−771 pg/mL), we suspected maternal VB_{12} deficiency, but her mother's serum VB_{12} level was normal. These biochemical findings persisted until the age of 47 days, when we started the administration of methylcobalamin (250 μg/day).

At the age of 2 months, her serum MMA level was nor-

Table 4. Clinical course of case 6. After methylcobalamin medication under suspicion of a vitamin B12 deficiency, serum MMA levels normalized but tHcy levels remained elevated. After betaine administration, plasma tHcy levels decreased.

DBS	day 4	day 20		day 20	day 47	2M	3M	5M
tHcy (≥ 5.0 μmol/L)	15.7	17.7	Plasma tHcy (≥ 10.0 μmol/L)	52.0	45.5	20.4	25.1	33.4
MMA (≥ 1.0 μmol/L)	<1.0	1.7	Serum MMA (≥ 1.0 μmol/L)	3.9	3.2	<1.0	<1.0	<1.0
Met (<10 μmol/L)	9.54	22.5	Plasma Met (<10.0 μmol/L)	28.6	28.2	35.0	18.5	21.5
			SerumVB12 (197−771 pg/mL)	146	141	5,618	7,590	6,467
			Serum folic acid (5.1−11.7 nmol/L)	7.6	7.8	7.6	7.1	5.8
				methylcobalamin				
				betaine				

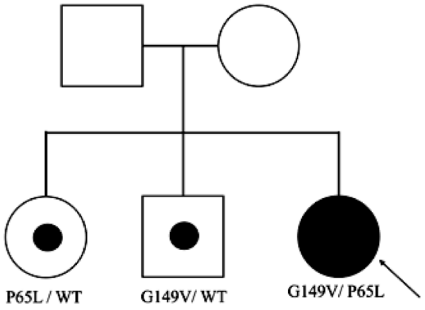

Fig. 1. Pedigree chart of case 6 that was confirmed to have MTHFR deficiency.
●: affected individual, ⊙ and ⊡: carriers.

mal, but plasma tHcy level remained slightly high (20.4 μmol/L). Gene panel analysis detected two missense *MTHFR* variants: p.P65L and p.G149V. Her sister was heterozygous for p.P65L, and her brother for p.G149V (Fig. 1) which was previously reported as a variant of the infantile onset type[10]. p.P65L is not registered in the Human Gene Mutation Database, but in silico analysis using PolyPhen-2 (http://genetics.bwh.harvard.edu/pph2/) suggested pathogenicity. Her MTHFR enzyme activity was 56.3 μU/mg protein in lymphocytes (8.4% of mean control value), 19.6 μU/mg protein in lymphoblast extracts (5.0% of mean control value), and 50.2 mmol/min/L in DBS (11.5% of mean control value). On the basis of these findings, we diagnosed late-onset MTHFR deficiency, and initiated betaine administration (100 mg/kg/day) at the age of 9 months. At the age of 10 months, she showed normal growth and development, with marker metabolite levels of tHcy 18.9 μmol/L and Met 30.5 μmol/L.

Discussion

HCU is classified into three forms. HCU type 1 is caused by cystathionine synthase deficiency, in which conversion of homocysteine to cystathionine is impaired and remethylation to methionine increases. HCU type 2 is caused by defects in the synthesis of methylcobalamin, which is a methyl donor in the reaction of methionine synthase. HCU type 3 results from MTHFR deficiency, in which the formation of 5′-methyltetrahydrofolate is impaired, causing methylcobalamin deficiency. Because the supply of Met from the remethylation of homocysteine is reduced in HCU types 2 and 3, they cannot be detected by the current NBS. In these forms of homocystinuria, betaine (N,N,N-trimethylglycine) can serve as another methyl donor instead of methylcobalamin as it is a substrate for betaine−homocysteine methyltransferase (BHMT). Though the physiological function of BHMT cannot compensate for methionine synthase which requires methylcobalamin, the pharmacological dosage of betaine can be sufficient to reduce tHcy and increase Met levels in the blood. Met is converted into S-adenosylmethionine (SAM), which is an important methyl donor for various methylation reactions. Therefore, maintaining normal levels of plasma Met is essential in preventing severe damage to the central nervous system caused by SAM deficiency, especially during infancy and childhood[1]. Because it has been shown that the early introduction of betaine therapy can suppress the symptoms of homocystinuria caused by remethylation defects[1–4], a highly preventive effect of NBS is expected.

MTHFR deficiency is known to present with a wide range of phenotypes. In severe cases, hydrocephalus, respiratory disorders, and epilepsy appear in the neonatal

period[11]. The disease prognosis can be greatly improved by the earliest introduction of betaine and other supplements, including folic acid, vitamin B_6, vitamin B_{12}, methionine and N^5-methyltetrahydrofolate. Among these therapeutics, betaine has been shown to be most effective in improving psychomotor development[4]. Prior to the present study, we treated two siblings with MTHFR deficiency. The proband presented with severe symptoms from the neonatal period. The diagnosis was confirmed at the age of 4 months. Betaine therapy was started and her condition improved remarkably, but severe neurological sequelae remained. The younger sibling was proved to be affected with the same disease soon after birth. Betaine therapy was started on the 7th day of life, and he remained asymptomatic until the last examination at the age of 6 years. Met levels in their newborn DBS were 6.6 and 8.7 μmol/L, respectively[1].

In the late-onset form of MTHFR deficiency, progressive polyneuropathy, cognitive impairment, seizures, and leukoencephalopathy become more pronounced after school age. However, it is often difficult to diagnose the disease because these symptoms are not very specific[12]. MTHFR enzyme activity in skin fibroblasts is estimated to be 10−20% in late-onset MTHFR deficiency[12]. The disease cannot be detected during the neonatal period using the current NBS in Japan, but in several countries, newborns presumed to have the late-onset form of disease were successfully found by detecting slightly elevated homocysteine levels in DBS[13].

In several studies on NBS for disorders of cobalamin metabolism[4,8,9], low Met levels with a cutoff of 8−11 μmol/L were used in the first-tier test. In our preliminary retrospective study on newborn DBS comparing performance of Met cutoff set at 9.0 μmol/L and 10.0 μmol/L, the positive rate increased significantly from 0.05% for the former to 0.12% for the latter[1]. Referring to the NBS data of the above-mentioned siblings, we set the Met cutoff for hypomethioninemia at 10 μmol/L in our prospective pilot NBS to ensure sufficient sensitivity.

In the current study, 267 (1.27%) of 21,105 enrolled newborns became positive in the first-tier tests, which reduced to six by the second-tier measurement of MMA and tHcy, representing a false positive rate in the first-tier tests of 97.8%. As second-tier tests are not financially supported in the current NBS program by the local governments, alternative ways to reduce the false positive rate in the first-tier tests must be found. Low-birth-weight infants and preterm infants were previously reported to show low Met levels in their blood[9], and similar tendencies were observed in our study (Table 3). In several countries where similar screening has been carried out, other markers such as ratio of Met/Phe are adopted in the first-tier tests. In our study, we observed a tendency for high Phe levels in infants with a birth weight ＜2,000 g. Based on these data, it is suggested that Met/Phe would not help to reduce the positive rate in NBS for hypomethioninemia. In the practice of current NBS in Japan, all newborns with a birth weight below 2,000 g are retested after their weight reaches 2,000 g. In our preliminary retrospective study, all the low-birth-weight infants who were assigned as positive for hypomethioninemia (Met ＜10 μmol/L) became negative in the retest after the above-mentioned weight gain. As a practical solution, infants with a birth weight ＜2,000 g who are positive for hypomethioninemia should be retested after their weight reaches 2,000 g so long as they remain free from symptoms indicative of remethylation disorders. When clinical changes are noticed, further evaluation should be started immediately. This scheme will enable to rule out most of false-positive results in the first-tier NBS without requiring the second-tier measurement of MMA and tHcy.

Conclusions

We conducted a pilot NBS program for disorders of cobalamin metabolism. The successful detection of a mild case of MTHFR deficiency suggests good sensitivity of C3, C3/C2, C3/Met, and low Met markers in combination, keeping appropriate specificity with second-tier measurements of tHcy and MMA. High false-positive rate for low Met that were mostly due to transient hypomethioninemia of low-birth-weight infants can also be resolved by retest after enough weight gain.

Acknowledgments

The authors would like to thank Professor Jin Osaka and Assistant Professor Kohei Sunoki (Department of Pediatrics, Jichi Medical University Hospital, Shimotsuke, Tochigi, Japan) for performing MTHFR activity analysis. The authors would like to thank the technicians at the Hiroshima City Medical Association Clinical Laboratory for performing the analysis of amino acids and acylcarnitines in DBS.

Institutional Review Board Statement

The study was conducted according to the guidelines of the Declaration of Helsinki, and was approved by the ethics committee of Hiroshima University (E2018-1522, 12 Dec 2020).

Informed Consent Statement

Informed consent was obtained from the parents of all the subjects enrolled in this study.

Conflicts of Interest

The authors declare no conflict of interest.

Funding

This study was partly supported by Children and Families Agency Program, Government of Japan (Grant Number 23DA0801, Chief Investigator: Go Tajima) and a grant from the Morinaga Hoshi-Kai Foundation.

References

1) Kagawa R, Tajima G, Maeda T, Utsunomiya AN, Hara K, et al: Pilot study on neonatal screening for methylmalonic acidemia caused by defects in the adenosylcobalamin synthesis pathway and homocystinuria caused by defects in homocysteine remethylation. *Int J Neonatal Screen* 7: 39, 2021.
2) Diekman EF, Koning TJ, Verhoeven-Duif NM, Rovers MM, Hasselt PM: Survival and psychomotor development with early betaine treatment in patients with severe methylenetetrahydrofolate reductase deficiency. *JAMA Neurol* 71: 188−194, 2014.
3) Nishimoto E, Ito Y, Sakakibara T, Nishiku T: Early treatment using betaine and methionine for a neonate with MTHFR deficiency. *Pediatrics Int* 61: 1265−1266, 2019.
4) Huemer M, Kožich V, Rinaldo P, Baumgartner MR, Merinero B: Newborn screening for homocystinurias and methylation disorders: systematic review and proposed guidelines. *J Inherit Metab Dis* 38(6): 1007−1019, 2015.
5) Adams JD, Bender HA, Miley-Åkerstedt A, Frempong T, Schrager NL, et al: Neurologic and neurodevelopmental phenotypes in young children with early-treated combined methylmalonic acidemia and homocystinuria, cobalamin C type. *Mol Genet Metab* 110: 241−247, 2014.
6) Shigematsu Y, Hirano S, Hata I, Tanaka Y, Sudo M, et al: Newborn mass screening and selective screening using electrospray tandem mass spectrometry in Japan. *J Chromatogr B Analyt Technol Biomed Life* 776(1): 39−48, 2002.
7) Shigematsu Y, Yuasa M, Ishige N, Nakajima H, Tajima G: Development of second-tier liquid chromatography-tandem mass spectrometry analysis for expanded newborn screening in Japan. *Int J Neonatal Screen* 7: 44, 2021.
8) Schnabel E, Kölker S, Gleich F, Feyh P, Hörster F, et al: Combined newborn screening allows comprehensive identification also of attenuated phenotypes for methylmalonic acidurias and homocystinuria. *Nutrients* 15: 3355, 2023.
9) Wong D, Tortorelli S, Bishop L, Sellars EA, Schimmenti LA, et al: Outcomes of four patients with homocysteine remethylation disorders detected by newborn screening. *Genet Med* 18: 162−167, 2016.
10) Weile J, Kishore N, Sun S, Maaieh R, Verby M, et al: Shifting landscapes of human MTHFR missense-variant effects. *Am J Hum Genet* 108: 1283−1300, 2021.
11) Goyette P, Christensen B, Rosenblatt DS, Rozen R: Severe and mild mutations in cis for the methylenetetrahydrofolate reductase (MTHFR) gene, and description of five novel mutations in MTHFR. *Am J Hum Genet* 59: 1268−1275, 1996.
12) Goyette P, Frosst P, Rosenblatt DS, Rozen R: Seven novel mutations in the methylenetetrahydrofolate reductase gene and genotype/ phenotype correlations in severe methylenetetrahydrofolate reductase deficiency. *Am J Hum Genet* 56: 1052−1059, 1995.
13) Barretta F, Uomo F, Fecarotta S, Albano L, Crisci D, et al: Contribution of genetic test to early diagnosis of methylenetetrahydrofolate reductase (MTHFR) deficiency: The experience of a reference center in southern Italy. *Genes* 14: 980, 2023.

Research Paper

Polyamine-based isolation of extracellular vesicles: Examination in suspension cells and mechanistic considerations

Arizumi Kikuchi[1,2], Motoki Mori[2], Yuria Tachibana[2], Azumi Naruse[1], Kenichi Nonaka[1,3], Kimiaki Takagi[4], Keiko Kano[5], Emi Mishiro-Sato[5], Kaname Tsutsumiuchi[2]*

[1]Daiyukai Research Institute for Medical Science, 25 Azaicho, Ichinomiya, Aichi 491−0113, Japan
[2]College of Bioscience and Biotechnology, Chubu University, 1200 Matsumoto, Kasugai, Aichi 487−8501, Japan
[3]Department of Surgery, Daiyukai General Hospital, 1−9−9 Sakura, Ichinomiya, Aichi 491−8551, Japan
[4]Department of Urology, Daiyukai General Hospital, 1−9−9 Sakura, Ichinomiya, Aichi 491−8551, Japan
[5]Institute of Transformative Bio-Molecules (WPI-ITbM), Nagoya University, Furo-cho, Chikusa, Nagoya 464−8601, Japan

Abstract We previously reported a novel method for isolating extracellular vesicles (EVs) using a polyamine solution through liquid chromatography-tandem mass spectrometry analysis of the culture supernatant of adherent cells, NCI-N87, and demonstrated its efficacy from multiple perspectives. Herein, K562 cells, a suspension cell line, were used to investigate the differences between the adherent cells. Furthermore, we elucidated the mechanism of EV isolation by focusing on the proteins' isoelectric point (pI) on the EV surface.

Samples were prepared using a conditioned medium from the NCI-N87 and K562 cell lines. The conditioned medium was analyzed after replacing the medium with a serum-free medium and culturing for 48 h. The polyamine precipitation (PA) method was compared with the ultracentrifugation (UC) method.

Using K562 cells, the recovery of EVs using the PA method allowed the detection of common EV marker proteins. The gene ontology analysis also indicated that EV-related terms ranked the highest, similar to the UC method. These results demonstrate that the PA method is also effective for recovering EVs from suspended cells, such as K562 cells.

When the average pI values were calculated with the abundance and the pI values for the surface proteins in the collected EVs, the values with the PA method were lower than those with the UC method. These results suggest that electrostatic interactions bring the easy recovery of EVs with polyamines.

Key words: extracellular vesicle, liquid biopsy, liquid chromatography-tandem mass spectrometry (LC-MS/MS), isoelectric point (pI), polyamine precipitation method

1. Introduction

1.1. Current status and issues surrounding the extracellular vesicles

Extracellular vesicles (EVs) are membrane-bound vesicles secreted by cells, including exosomes, microvesicles, and apoptotic bodies[1)]. These vesicles play a crucial role in intercellular communication and have been reported to be useful diagnostic tools in various medical fields, including liquid biopsy[2)]. Because of their small size and low immunogenicity, EVs are also being explored for drug delivery and therapeutic applications, with great promise for practical applications in cancer, regenerative medicine, and gene therapy[3)].

In addition to their medical applications, EVs are gaining attention in agriculture, environmental science, the food industry, and cosmetics. In the food industry, there is ongoing research into developing foods that deliver nutritional

* **Corresponding author**
Kaname Tsutsumiuchi
College of Bioscience and Biotechnology, Chubu University, 1200 Matsumoto, Kasugai, Aichi 487−8501, Japan
Tel: +81−568−51−6295, Fax: +81−568−52−6594
E-mail: tsutsu@fsc.chubu.ac.jp
Received: February 14, 2025. Accepted: May 21, 2025.
Epub June 6, 2025.
DOI: 10.24508/mms.2025.06.004

and functional components to target areas in the body[4,5]. In the cosmetics field, the application of EVs for skin care and anti-aging is being explored, with studies examining their effectiveness in promoting skin regeneration and preventing aging, focusing on the efficacy of promoting skin regeneration and preventing aging[6,7].

Several methods have been reported and implemented to isolate EVs. Accurate isolation and characterization of EVs are critical in their analysis, and each method has its characteristics, with the choice depending on the intended purpose[8]. The ultracentrifugation (UC) method is the most frequently used EV isolation method and is considered the gold standard[9]. Although it can be used with various samples, it requires specialized equipment, and there are concerns about the purity of the isolated EVs[9].

Other methods include polymer precipitation, size-exclusion chromatography (SEC), and immunoaffinity capture (IC). Polymer precipitation is easy to perform and allows for quick recovery, but it has low purity owing to residual polymers and protein contamination[10]. SEC and IC methods produce purer EVs with fewer impurities, but they are not suitable for large sample volumes and are costly[10]. Microfluidic devices represent a novel method for the efficient and rapid isolation of EVs. These devices allow for the quick and high-precision separation of EVs through microscopic channels, yielding high-purity EVs even from small sample volumes. However, they require specialized devices, have high installation costs, and are not yet widely standardized commercially[11].

Another method involves antibodies against specific markers or lipid components on the EV surface. Magnetic bead separation is a common technique in this category, offering high specificity and the ability to isolate the target EVs selectively. However, this method is challenging in terms of cost and sample volume and cannot recover EVs that do not have specific markers[12].

Each EV isolation method has advantages and disadvantages. Obtaining sufficient amounts of EVs may be challenging, particularly when limited clinical samples are used. When isolating EVs, considering various aspects such as the sample volume, simplicity of the procedure, level of purity in the extracted EVs, and associated expenses is crucial. Additionally, employing standardized techniques is essential to guarantee consistent isolation results.

Our research focuses on a novel approach for EVs utilizing a polyamine solution called the PA method. We examined this innovative technique for EV isolation. We presented the findings from liquid chromatography-mass spectrometry (LC-MS/MS) analysis conducted on a conditioned medium obtained from the NCI-N87 adherent cell line[13].

1.2. Outline of the assumed PA method

An outline of the proposed PA method is shown in Fig. 1. The method comprises adding the NaCl and polyamine solution, mixing, and allowing the mixture to stand. After centrifugation, the supernatant was removed, and the samples were analyzed.

The PA method is characterized by the fact that it does not require any special equipment and can be performed using an ordinary centrifuge. Furthermore, the polyamine solution used is inexpensive and readily available.

In this study, we present the results of various analyses using K562 cells, which are floating cells, not adherent

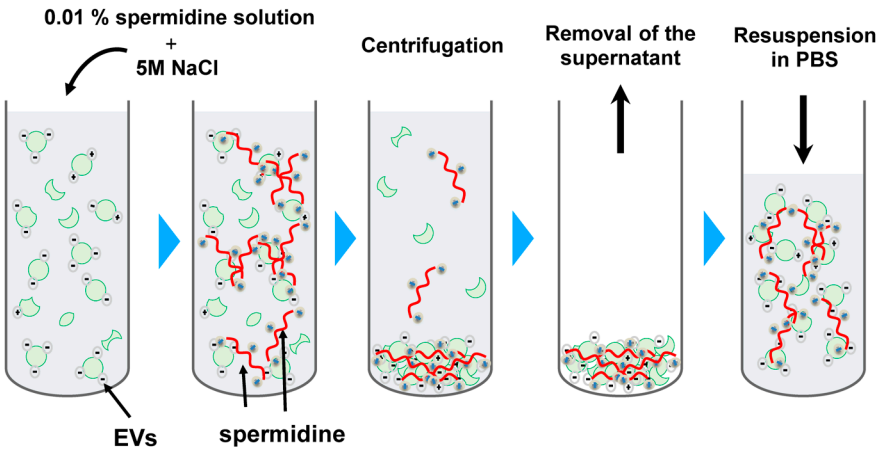

Fig. 1. Overview of the PA method.

cells, and compare them with NCI-N87. Furthermore, we focused on the reaction mechanism of the PA method, specifically examining the protein charge (pI) present in the membrane of EVs, and performed multiple studies using the pI of NCI-N87 (adherent cells) and K562 (suspended cells).

2. Materials and Methods

2.1. Cell culture

Two cell lines were utilized for LC-MS/MS analysis: NCI-N87 (ATCC, Manassas, VA, USA) and K562 (National Institute of Biomedical Innovation, Health and Nutrition, Osaka, Japan). The cells were cultured in RPMI-1640 Medium supplemented with L-Glutamine and Phenol Red (Fujifilm Wako, Tokyo, Japan), along with 10% fetal bovine serum, at 37˚C in a 5% CO_2 incubator. Upon reaching confluence, the medium was replaced with an Advanced RPMI 1640 Medium (Thermo Fisher Scientific, Waltham, MA, USA). After 48 h of culture, the media were collected and subjected to initial centrifugation at 1,000 × *g* for 10 min at room temperature (20−25˚C) to pellet and remove any cells. All subsequent centrifugation steps were performed at 4˚C. The supernatant was then centrifuged at 2,000 × *g* for 20 min. Following centrifugation, the media supernatant was filtered through a 0.22-μm pore filter (HAWACH Scientific Co. LTD, Xian City, China). Each procedure was conducted using a prefiltered culture medium.

2.2. EVs isolation

2.2.1. Ultracentrifugation

To isolate EVs, we removed the cells and subjected the prefiltered culture supernatant_to ultracentrifugation. This procedure was performed utilizing an Optima L-90K ultracentrifuge (Beckman Coulter, Fullerton, CA, USA) at 150,000 × *g* for 100 min with an SW28.1 swinging bucket rotor (Beckman Coulter). After the initial centrifugation, phosphate-buffered saline (PBS) was introduced into the upper portion of the centrifuge tube (17 mL, Open-Top Thin wall_Ultra-Clean Tube (Beckman Coulter), and the ultracentrifugation process was repeated under identical conditions. The supernatant was discarded, and the isolated EVs were resuspended in PBS.

2.2.2. Polyamine precipitation (PA) Method

For the PA method, the treated cell culture supernatant was transferred into a 15 mL conical centrifuge tube (Nunc, Thermo Fisher Scientific, USA). A 1/10 volume of 5 M NaCl solution and a 1/10 volume containing 0.01% spermidine (191-13831, FUJIFILM Wako Chemicals, Osaka, Japan) were added to the supernatant. The mixture was subsequently incubated for 10 min at room temperature before centrifugation at 27,210 × *g* (13,000 rpm) for 60 min in a refrigerated microcentrifuge (Model 3700; KUBOTA CORPORATION, Tokyo, Japan). The supernatant was discarded following centrifugation, and the EVs were resuspended to PBS for subsequent analysis.

2.3. Mass spectrometry

2.3.1. Sample preparation

Samples containing EVs collected using the PA or UC method were treated with single-pot solid-phase-enhanced sample preparation (SP3) technology. The protein concentration in the sample was adjusted to 1−200 μg/mL, and dithiothreitol was added to achieve a final concentration of 25 mM. The sample was subsequently incubated at room temperature for 30 min, followed by adding 1/10 volume of 500 mM 3-methyl-1-butanol and further incubation for 30 min. Subsequently, Sera-Mag™ SpeedBead Carboxylate-Modified [E3] Magnetic Particles (Global Life Sciences Technologies Japan K.K., Tokyo, Japan) were introduced into the samples at a volume of 10 μL for every 10 μg of protein. Then, ethanol was added three times to the sample volume, and the mixture was agitated at 1,000 rpm for 10 min at room temperature. The sample was washed thrice with 80% ethanol (500 μL) using a magnetic stand. In conjunction with 50 mM Tris buffer, lysyl endopeptidase was introduced (100 μL) into the washed sample, which was then sonicated and incubated at 37˚C for 3 h. Trypsin was subsequently added, and the sample was mixed at 1,500 rpm at 37˚C for 20 h. Following digestion, 20% trifluoroacetic acid was added to achieve a final concentration of 1/20 of the volume, and the magnetic particles were separated. The supernatant was collected, desalted using GL-Tip SDB (GL Sciences Inc., Tokyo, Japan), vacuum-dried, and resuspended in 0.1% trifluoroacetic acid with 2% acetonitrile to facilitate peptide extraction.

2.3.2. LC-MS/MS analysis

LC-MS/MS analysis was conducted using a PAL System autosampler (CTC Analytics AG, Zwingen, Switzerland) and a Q Exactive Hybrid Quadrupole-Orbitrap Mass Spec-

trometer (Thermo Fisher Scientific). The peptides were concentrated on a C18 trap column (5-μm particle size, 300 μm inner diameter, 5 mm length; Chemical Evaluation and Research Institute, Tokyo, Japan) and subsequently separated on a C18 analytical column (3-μm particle size, 100-μm inner diameter, 125 mm length; Nikkyo Technos, Tokyo, Japan) at a flow rate of 0.5 μL/min, with an injection volume of 7.5 μL. The mobile phases were solvent A (0.5% acetic acid) and solvent B (0.5% acetic acid in 80% acetonitrile). The gradient elution for solvent B commenced at 5%, increased to 40% over 100 min, increased to 95% over 1 min, maintained at 95% for 3 min, returned to 5% over 1 min, and equilibrated at 5% for 10 min. Electrospray ionization was performed in positive ion mode. The mass spectrometer was operated in data-dependent acquisition (DDA) mode. The peptide spectra were acquired using Xcalibur 4.1.50 software (Thermo Fisher Scientific). Full scans were recorded from 350 to 1,800 *m/z* at a resolution of 17,500, with an automatic gain control (AGC) target of 3×10^6 and a maximum injection time of 60 ms. MS/MS scans were performed at a resolution of 35,000 with an AGC target of 1×10^5 and a maximum injection time of 60 ms. The 10 most intense precursor ions were selected for MS/MS analysis in the quadrupole with an isolation window of 2.0 *m/z* and fragmented via higher-energy collisional dissociation (HCD) using a normalized collision energy of 27%. Multiply-charged peptides were prioritized for MS/MS with a dynamic exclusion set to 20 s.

2.3.3. Data analysis

The protein sequence database used for the analysis was UniProt Homo sapiens (TaxID=9,606), downloaded on September 24, 2022, in conjunction with the cRAP contaminant database (http://www.thegpm.org/crap/). Proteome Discoverer 2.5.0.400 (Thermo Fisher Scientific) was employed for data analysis, and SEQUEST (Thermo Fisher Scientific) was utilized for database searches. The search parameters were configured to allow for two missed cleavage sites with a peptide mass tolerance of 10 ppm and a fragment mass tolerance of 0.02 Da. Fixed modifications included the carbamidomethylation of cysteine, whereas variable modifications included methionine oxidation and N-terminal acetylation. Peptide identifications were filtered using significant Xcorr values with a false discovery rate of 1% based on the Percolator node in Proteome Discoverer. The mass spectrometry data were deposited in the jPOST[14] repository (project ID: JPST001807, accession ID: PXD PXD035832 for NCI-N87; project ID: JPST003429, accession ID: PXD056938 for K562).

2.4. Analysis of the K562 cells culture supernatant

Furthermore, proteins specified in the MISEV2023 guidelines[15] were evaluated for their presence in the sample, and significant peptide spectrum matches (PSMs) were identified. A comparative analysis between the PA and UC methods was carried out using total ion chromatograms, diagrams, and volcano plots to assess the recovered peptides' concordance rates and distinctive characteristics.

Volcano plot analysis was conducted on the proteins obtained using the PA and UC methods. The tetraspanin markers CD9, 63, 81, and Flotillin 1, which are frequently utilized in EV analysis, were examined. Additionally, four markers, actin, EMMPRIN, HSPA8, and HAP90AB1, were selected from the proteins enumerated in MISEV2023 that exhibited PSMs $\geq$ 4 using both methods and were subsequently analyzed. Gene Ontology (GO) analysis for cellular components was performed on proteins detected using both methods, focusing on PSMs with a mean of 4 or higher. The analysis was conducted using the DAVID program (v2024q1)[16].

Among the proteins detected, the correlation between the two methods was examined for those with PSMs greater than 4.0.

2.5. Analysis using the pI of EVs membrane proteins

This study focused on the analysis of proteins localized to the EVs membrane. The target proteins were aggregated and cataloged based on information about the EV membrane surface utilizing GO terms from Metascape[17]. Consequently, 57 proteins were selected for analysis. The cumulative abundance values of these proteins were calculated for pI ranges from 4.5 to 11.5 in increments of 1.0. Furthermore, for proteins detected using both the PA and UC methods with PSMs $\geq$ 4, the cumulative values of their pI and abundance were calculated using the following formula:

$$\frac{\sum_{pI=4}^{12}(pI \times Abundance_{pI})}{\sum_{pI=4}^{12}(Abundance_{pI})}$$

The sum of the product of pI and the abundance for each detected protein was subsequently indexed by dividing the sum of the pI and the abundance by the sum of the abundance.

3. Results

3.1. Performance evaluation of the PA method using K562 cells

Table S1 summarizes the protein data obtained with both methods using the K562 cell content detection data as the protein content-EVs characteristics for PSMs greater than 4. With the PSMs using K562, the correlation coefficient for both methods was R^2=0.646, and the overall correlation was positive, as shown in Fig. 2.

Fig. 3 shows the total ion chromatograms using K562. Each method showed a different profile even though the same samples were treated using the PA and UC methods.

A volcano plot obtained using the K562 cells is shown in Fig. 4. The results for the examined tetraspanin markers and other markers are shown. Table S2 lists the proteins used in the analysis, including the quantitative information.

In the GO analysis, EV markers, including exosomes, accounted for the highest annotation cluster and were enriched; enrichment scores for the PA and UC methods were 171.7 and 176.5, respectively (Table S3).

3.2. Performance evaluation of the PA method using K562 cells

The membrane proteins selected for analysis are listed in Table S4. The pI values were 6.30±1.20. The correlation between the cumulative abundance values and pI for NCI-N87 is shown in Fig. 5(a) and for K562 in Fig. 5(b). The comparison of the total abundance was different between NCI-N87 and K562 cells. However, when comparing the average cumulative pI values at pI ≥ 4, K562 cells exhibited 6.05 for the PA method and 6.35 for the UC method, whereas NCI-N87 cells displayed values of 6.18, PA method, and 7.02, respectively. For the UC method, when pI was 4 or higher, the values for K562 cells were 6.08 and 6.37, and for NCI-N87 cells, the values were 5.83 and 7.13. When considering both methods with pI values of 4 or higher, the values for K562 cells were 6.07 for the PA method and 6.35 for the UC method, and for NCI-N87 cells, the values were 5.80 for the PA method and 7.10 for the UC method. In all the cases, the PA method yielded lower values.

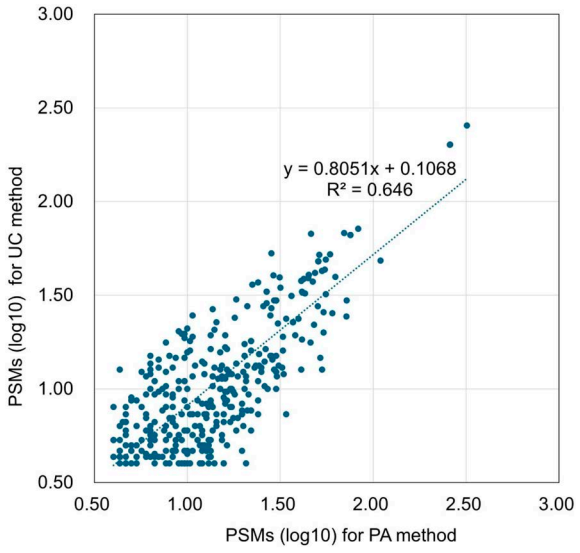

Fig. 2. Relationship between the PA method and the UC method for PSMs using K562.
The x-axis represents the PA method, and the y-axis represents the UC method.

4. Discussion

Herein, we investigated the recovery of EVs using the PA method and their protein composition using LC-MS/MS in the suspension cell line K562. Initially, as observed with NCI-N87, an adherent cell line, the ion chromatograms obtained from K562 cells showed differences between the two methods. Volcano Plot analysis revealed that, unlike NCI-N87, the EV markers with the PA method were less than those with the UC method. This discrepancy may be attributed to the influence of debris generated during the suspension cell culture process, in addition to the presence of a specific factor related to K562 cells, which was the subject of this investigation.

In the GO analysis, analogous to the results obtained using NCI-N87, the terms associated with EVs demonstrated the highest rank, as observed in the UC method. Additionally, the two methods positively correlated with the proteins detected with PSMs ≥ 4.0. These findings suggest that the PA method could be used to recover EVs. On the other hand, the relationship between pI and cumulative abundance for surface proteins in collected EVs from NCI-N87 (Fig. 5(a)) and K562 (Fig. 5(b)) revealed that the averages of pI values with the PA method were lower than those with the UC method. These observations indicate that polyanionic EVs may aggregate through electrostatic interactions with polyamines, which are polycations, and that the PA method can recover a protein population specific to EVs compared with the conventional UC method. Notably, this method is particularly effective for analyzing EV proteins in the low-pI range.

EVs in liquid biopsies can be important information

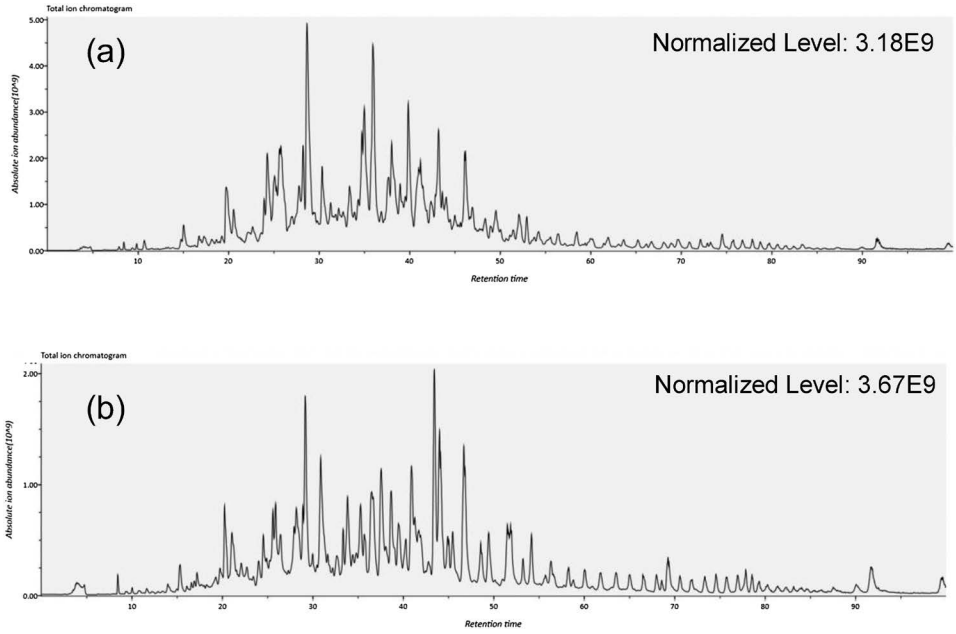

Fig. 3. Comparison of the PA method and UC method using the total ion chromatogram using K562.
(a) PA method, (b) UC method.

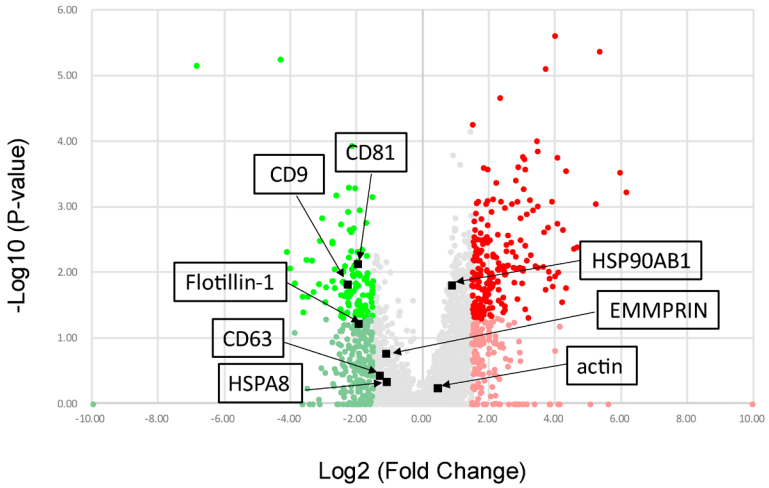

Fig. 4. Volcano plot for each method.
Marked for proteins in EVs at K562. Created using abundance data obtained by LC-MS/MS. The x-axis indicates the log2 fold change for each gene, and the y axis indicates the log10 p-value. Red dots indicate proteins with p-values <0.05, and green dots indicate proteins with p-values ≥ 0.05. The significance of differences was evaluated using t-test, with p-value <0.05 being significant.

sources for cancer diagnosis and treatment monitoring[18]. Tumor-derived EVs often contain tumor-specific biomarkers that aid in tracking cancer progression and treatment response[19]. Furthermore, the stability of EVs as biomarkers is notable because their lipid bilayer protects their contents, making them suitable for analysis[20]. Analysis of the contents of EVs can reveal the genetic characteristics and molecular mechanisms of cancer, thereby contributing to personalized medicine. Thus, EVs are expected to be valuable tools in liquid biopsies for cancer diagnosis and treatment monitoring.

To investigate the reaction mechanism of the PA method, we focused on the pI and found that the PA method recovered proteins with lower pI values than the UC method.

Exosomes in EVs are surrounded by a phospholipid bilayer containing negatively charged phosphate groups[21]. These phosphates provide the exosome surface with a negative charge[22, 23]. In addition, surface proteins and glycans on exosomal membranes contribute to the anionic nature of exosomes[24]. Exosomes play a role in intercellular communication, and their negative charge facilitates interactions with cationic (positively charged) regions on the recipient

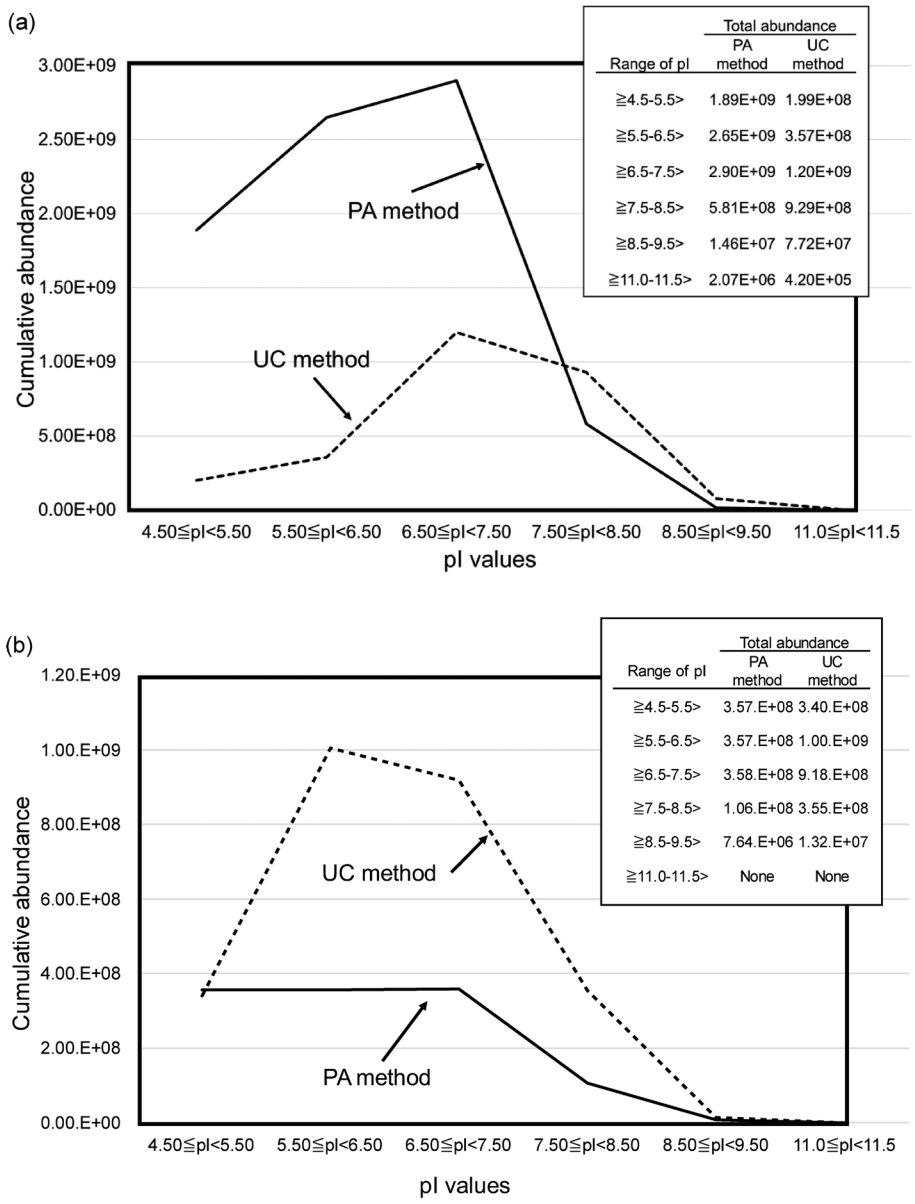

Fig. 5. Relationship between pI and cumulative abundance for surface proteins in collected EVs.
(a) NCI-N87, (b) K562.
The y-axis represents the cumulative abundance, and the x-axis represents the pI value, which was set in the range of 4.5 to 11.5.

cell surfaces[25].

The PA method is based on the electrical properties of the polyamines. In other words, an ion complex considerably forms between EVs and polyamines to form a coacervate[26]. Various free proteins in the culture medium are also assumed to form ion complexes with polyamines because they exist in a random coil state and have a negative charge. We consider that concerning the proteins detected by the UC method, a high concentration of NaCl in the reaction solution prevents coacervate formation in those with small particle sizes and low charge densities. However, further studies are required to confirm these findings.

While this study was a basic examination using culture supernatants, we aimed to conduct further research using clinical specimens to explore the potential for the clinical application of the PA method.

Conclusions

A study using the culture supernatant from the suspension cell line K562 and analyzed by LC-MS/MS demonstrated that the PA method is a practical approach for EV recovery. Analysis of the pI suggests that the interaction occurs because of the charge properties of the polyamines and EVs.

Conflict of Interest

The authors declare that they have no conflicts of interest.

Supplementary material: additional data and analysis

Table S1. Protein content using the PA and UC methods analyzed by LC-MS/MS

PA method (a) and (b) UC method. The analysis was conducted in triplicate (N=3), and the list was composed of PSMs (peptide spectrum matches) with an average value of 4 or higher across any of the methods. Data are presented as means with standard deviations.

Table S2. List of proteins used in the volcano plot analysis

A. All proteins

B. Down regulated proteins

C. Up regulated proteins

Table S3. gene ontology (GO) classification

A. PA method

B. UC method

Table S4. Proteins on the membrane of the selected EVs

Gene symbol, accession number, and pI value are shown.

References

1) Xu R, Rai A, Chen M, Suwakulsiri W, Greening DW: Extracellular vesicle in cancer—Implications for future improvements in cancer care. *Nat. Rev. Clin. Oncol* 10: 617−638, 2018.
2) Yoshioka Y, Katsuda T, Ochiya T: Extracellular vesicles and encapusulated miRNAs as emerging cancer biomarkers for novel liquid biopsy. *Jpn J Clin Oncol* 48: 869−876, 2018.
3) Mosquera-Heredia MI, Morales LC, Vidal OM, Barceló E, Silvera-Redondo C, et al: Exosomes: Potential disease biomarkers and new therapeutic targets. *Biomedicines* 9: 1061, 2021.
4) Baier SR, Nguyen C, Xie F, Wood JR2, Zempleni J: MicroRNAs are absorbed in biologically meaningful amounts from nutritionally relevant doses of cow milk and affect gene expression in peripheral blood mononuclear cells, HEK-293 kidney cell cultures, and mouse livers. *J Nutr* 144: 1495−1500, 2014.
5) Ju S, Mu J, Dokland T, Zhuang X, Wang Q, et al: Grape exosome-like nanoparticles induce intestinal stem cells and protect mice from DSS-induced colitis. *Mol Ther* 21: 1345−1357, 2013.
6) Wu JY, Wu SN, Zhang LP, Zhao XS, Li Y, et al: Stem cell-derived exosomes: A new method for reversing skin aging. *Tissue Eng Regen Med* 19: 961−968, 2022.
7) Yang GH, Lee YB, Kang D, Choi E, Nam Y, Lee KH, et al: Overcome the barriers of the skin: exosome therapy. *Biomater Res* 25: 22, 2021.
8) Brennan K, Martin K, FitzGerald SP, O'Sullivan J, Wu Y, et al: A comparison of methods for the isolation and separation of extracellular vesicles from protein and lipid particles in human serum. *Sci Rep* 10: 1039, 2020.
9) Royo F, Théry C, Falcón−Pérez JM, Nieuwland R, Witwer KW: Methods for separation and characterization of extracellular vesicle: Results of a worldwide survey performed by the ISEV rigor and standardization subcommittee. *Cells* 9: 1955, 2020.
10) Gao J, Li A, Hu J, Feng L, Liu L, Shen Z: Recent developments in isolating methods for exosomes. *Front Bioeng Biotechnol* 10: 1100892, 2023.
11) Wu Y, Wang Y, Lu Y, Luo X, Huang Y, et al: Microfluidic Technology for the Isolation and Analysis of Exosomes. *Micromachines* 15: 630, 2024.
12) Nakai W, Yoshida T, Diez D, Miyatake Y, Nishibu T, et al: A novel affinity-based method for the isolation of highly purified extracellular vesicles. *Sci Rep* 6: 33935, 2016.
13) Kikuchi A, Naruse A, Nonaka K, Mori M, Yamada M, et al: Recovery of extracellular vesicles from liquid samples using polyamine solution. *Medical Mass Spectrometry* 8: 35−42, 2024.
14) Okuda S, Watanabe Y, Moriya Y, Kawano S, Yamamoto T, et al: jPOSTrepo: An international standard data repository for proteomes. *Nucleic Acid Res* 45(D1): D1107–D1111, 2017.
15) Welsh JA, Goberdhan DCI, O'Driscoll L, Buzas EI, Blenkiron C, et al: Minimal information for studies of extracellular vesicles (MISEV2023): From basic to advanced approaches. *J Extracell Vesicles* 13: e12404, 2024.
16) Sherman BT, Hao M, Qiu J, Jiao X, Baseler MW, et al: DAVID: A web server for functional enrichment analysis and functional annotation of gene lists (2021 update). *Nucleic Acid Res* 50(W1): W216–W221, 2022.
17) Zhou Y, Zhou B, Pache L, Chang M, Khodabakhshi AH, et al: Metascape provides a biologist-oriented resource for the analysis of systems-level datasets. *Nat Commun* 10:

1523, 2019.

18) Brennan K, Martin K, FitzGerald SP, O'Sullivan J, Wun Y, et al: A comparison of methods for the isolation and separation of extracellular vesicles from protein and lipid particles in human serum: *Sci Rep* 10: 1039, 2020.

19) Dabral P, Bhasin N, Ranjan M, Makhlouf MM, Elmageed XYA: Tumor-derived extracellular vesicles as liquid biopsy for diagnosis and prognosis of solid tumors: their clinical utility and reliability as tumor biomarkers. *Cancers* 16, 2462, 2024.

20) Boukouris S, Mathivanan S: Exosomes in bodily fluids are a highly stable resource of disease biomarkers. *Proteomics Clin Appl* 3−4: 358−367, 2015.

21) Skotland T, Hessvik NP, Sandvig K, Llorente A: Exosomal lipid composition and the role of ether lipids and phosphoinositides in exosome biology: *J Lipid Res* 60: 9−18. 2019.

22) Ghadami S, Dellinger K: The lipid composition of extracellular vesicles: applications in diagnostics and therapeutic delivery. *Front Mol Biosci* 10: 1198044. 2023.

23) Kosutova N, Lorencova L, Hires M, Jane E, Orovcik L, et al: Negative charge-carrying glycans attached to exosomes as novel liquid biopsy marker. *Sensors (Basel)* 24, 1128, 2024.

24) Hallal S, Tűzesi Á, Grau GE, Buckland ME, Alexander KL: Understanding the extracellular vesicle surface for clinical molecular biology. *J Extracell Vesicles* 11: e12260, 2022.

25) Nail HM, Chiu C-C, Leung C-H, Ahmed MMM, Wang Hui-Min D: Exosomal miRNA-mediated intercellular communications and immunomodulatory effects in tumor microenvironments: *J Biomed Sci* 30: 69, 2023.

26) Tsutsumiuchi K, Aoi K, Okada M: Ion complex formation between poly(amido amine) dendrimer HCl salt and poly(L-glutamic acid) sodium salt. *Polym J* 32: 107−112, 2000.

Short Communication

A case of primary meningococcal conjunctivitis in a young Japanese man rapidly identified as *Neisseria meningitidis* by MALDI-TOF MS

Noriko Mukai[1, 2*], Yukiya Takeichi[2], Yamato Yoshikawa[3], Kensuke Tajiri[2], Toyofumi Nakanishi[4], Teruyo Kida[2]

[1] Department of Ophthalmology, Hirakata City Hospital, 2−14−1 Kinyahonmachi, Hirakata, Osaka 573−1013, Japan
[2] Department of Ophthalmology, Osaka Medical and Pharmaceutical University, 2−7 Daigaku-machi, Takatsuki, Osaka 569−8686, Japan
[3] Yoshikawa Eye Clinic, 1−5 Kizuekimae, Kizugawa, Kyoto 619−0214, Japan
[4] Department of Medical Technology, Faculty of Medical Science, Shubun University, 6 Nikko-cho, Ichinomiya, Aichi 491−0938, Japan

Abstract We report a rare case of keratoconjunctivitis in a young Japanese man rapidly identified as *Neisseria meningitidis* by MALDI-TOF MS (matrix-assisted laser desorption-ionization time-of-flight mass spectrometry). The patient was diagnosed with primary meningococcal conjunctivitis. A 26-year-old man presented to Osaka Medical and Pharmaceutical University with a 3-day history of sudden pain onset in both eyes, conjunctival redness, tearing, and purulent eye discharge. The bulbar and palpebral conjunctiva were hyperemic and thickened, with superficial punctate keratitis in both eyes, and an area of stromal infiltration in the left eye. No epithelial defects or corneal thinning were observed. He had a slight fever and fatigue. Initial Gram staining of the conjunctiva revealed gram-negative diplococci, and, he had a sexual encounter two weeks ago, therefore, we suspected gonococcal conjunctivitis. The patient was administered with 1 g of intravenous ceftriaxone every 12 h for 7 days, and topical cefmenoxime hydrochloride and topical gatifloxacin hydrate were administered eight times per day. His condition improved dramatically after treatment; however, on the third day after admission, Neisseria meningitidis was detected through conjunctival swab culture and biochemical testing using the VITEK®2 NH card. We also rapidly identified *Neisseria meningitidis* through conjunctival swab mass spectrometry using matrix-assisted laser desorption/ionization time-of-flight mass spectrometry (MALDI-TOF MS). Later, the same bacterium was detected through genetic analyses. Following advice from our hospital's infectious disease control office, our patient was isolated in a private room for 1 week, and individuals who were in close contact with him were administered ciprofloxacin tablets. We strongly suspected gonococcal infection and initiated treatment, but *Neisseria meningitidis* was rapidly identified using conjunctival swab MALDI-TOF MS analysis. Therefore, appropriate treatment and infection prevention measures were possible.

Key words: *Neisseria meningitidis*, primary meningococcal conjunctivitis, matrix-assisted laser desorption-ionization time-of-flight mass spectrometry, gene sequence analysis

Introduction

Neisseria meningitidis is a gram-negative diplococcus that colonizes the nasopharyngeal mucosa and is transmitted via droplet infections from carriers or patients. In addition, it causes serious diseases, such as upper respiratory inflammation, pneumonia, urethritis, arthritis, pericarditis, bacteremia, and sepsis. Generally, meningococcal conjunctivitis can be classified as a primary or secondary systemic disease. Primary meningococcal conjunctivitis (PMC) is a rare cause of pediatric acute purulent bacterial conjunctivitis that is more frequently prevalent in children than in adults[1, 2]. Here, we report a rare case of PMC in a young Japanese adult who presented with clinical symptoms

*Corresponding author
Noriko Mukai
Department of Ophthalmology, Hirakata City Hospital, 2−14−1 Kinyahonmachi, Hirakata, Osaka 573−1013, Japan
Tel: +81−72−847−2821, Fax: +81−72−847−2825
E-mail: mukanori@kcn.jp
Received: April 30, 2024. Accepted: December 24, 2024.
Epub March 10, 2025.
DOI: 10.24508/mms.2025.06.001

resembling gonococcal keratoconjunctivitis. We could rapidly identify PMC pathogenetic microorganism on conjunctival swabs from this patient by matrix-assisted laser desorption/ionization time-of-flight mass spectrometry (MALDI-TOF MS). Significant advances in microbiological methods have been through achieved innovation in mass spectrometry[3]. MALDI-TOF MS has become the standard for microbial identification, enabling microbiology laboratories to reliably, rapidly, and cost-effectively identify starting from colony material[4]. This is also the case in our hospital. In this case as well, we were able to make a definitive diagnosis and administer appropriate treatment for this patient by MALDI-TOF MS analysis and genetic analyses.

Case report

A 26-year-old man was referred to a specialized outpatient ophthalmology clinic at our hospital because of persistent conjunctival hyperemia with purulent eye discharge under the suspicion of gonococcal conjunctivitis following sexual intercourse with an unidentified woman 2 weeks prior. He had been treated with antibiotic eye drops for conjunctivitis at another eye clinic; however, his condition deteriorated. During the initial visit to our department, the best-corrected visual acuity and intraocular pressure were not measurable because he was unable to keep his eyes open due to severe pain in both eyes. Both eyes were injected with marked discharge from both eyelids (Fig. 1a, b). The bulbar and palpebral conjunctiva showed hyperemia and thickening (Fig. 1c, d), accompanied by superficial punctate keratitis in both eyes and an area of stromal infiltrate in the left eye. The posterior segments of both the eyes were unremarkable. In terms of systemic symptoms, he had a slight fever and fatigue without headache or a stiff neck. Blood tests revealed only mildly elevated C-reactive protein levels. He also had a history of bronchial asthma. Subsequently, a conjunctival swab smear test was quickly performed, and gram-negative diplococci were detected (Fig. 2). Based on his clinical findings and sexual history, gonococcal conjunctivitis was strongly suspected. Therefore, 1 g of intravenous ceftriaxone was started every 12 h for 7 days, and topical cefmenoxime hydrochloride and gatifloxacin hydrate were administered eight times per day at our hospital. Although the ocular findings improved, meningococcus was identified by culture and biochemical testing using the VITEK®2 NH card three days after admission. Since adult case of PMC are rare in Japan and the results were unexpected, we additionally performed conjunctival swab MALDI-TOF MS. *Neisseria meningitidis* was rapidly identified. Furthermore, we conducted gene sequence analysis using conjunctival swabs to confirm the presence identify the same bacterium.

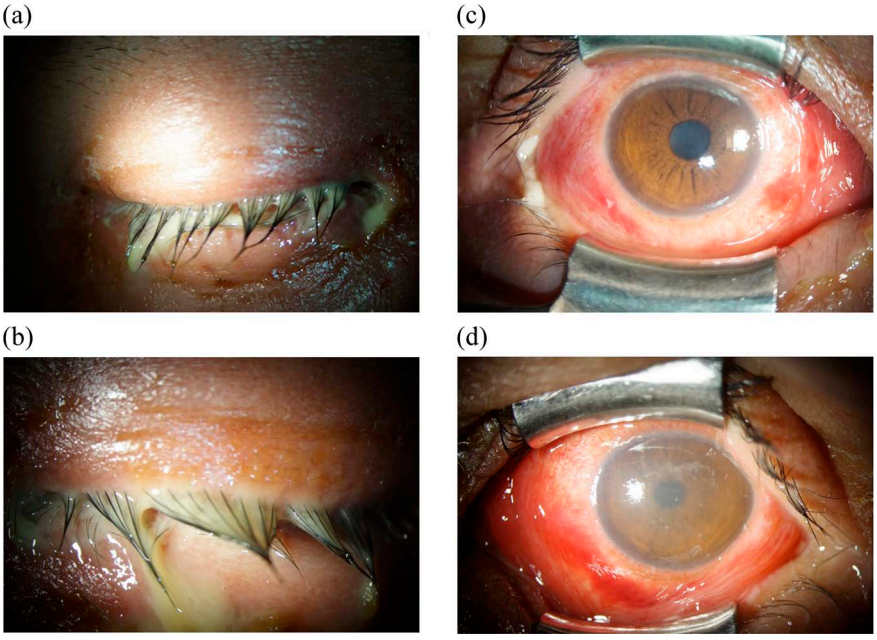

Fig. 1. Slit lamp photograph of the patient.
Slit lamp photograph shows a marked purulent discharge in the eyelids of right eye (a) and left eye (b). Slit lamp photograph shows the bulbar and palpebral conjunctiva presenting with hyperemia and thickening in right eye (c) and left eye (d).

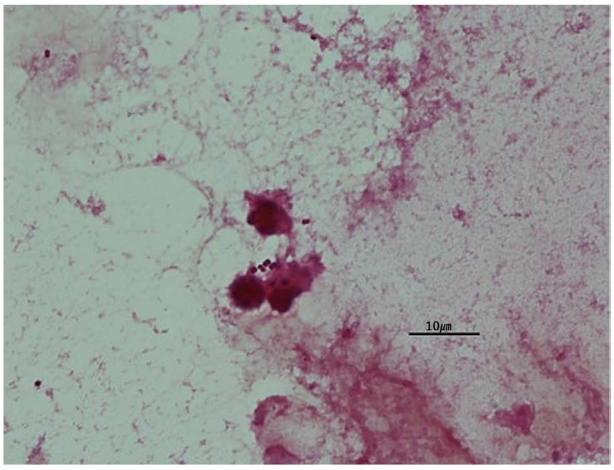

Fig. 2. Gram stain of the conjunctival swab characteristic of gram-negative diplococci polymorphs.

Materials and methods

Proteome analysis using MALDI-TOF MS was attempted to rapidly identify pathogenic microorganisms on conjunctival swabs from this patient. We applied matrix-assisted laser desorption/ionization time-of-flight mass spectrometry (MALDI-TOF MS) using a Linear mode, and identification was performed with the Biotyper software 3.0 program (Bruker Daltonics, Billerica, USA). The colonies were scraped off, directly placed on a MALDI plate, and then drying, 1 μL of pellets on the α-cyano-4-hydroxycinnamic acid (HCCA)-Matrix, we measured the MS. We checked the *m/z* calibration with the MBT calibrator (Bruker Daltonics KK., Tokyo) before MS analysis. The MS was carried out in the Autoflex-Speed using the Linear mode, and the results were analyzed using the Biotyper™ software 3.0 program (Bruker Daltonics, Billerica, USA).

All reagents except the HCCA were purchased from Nakalei tasque (Tokyo).

16S rRNA PCR amplification was performed for species identification according to the instruction manual from Nippon Gene Co., Ltd. PCR products were separated by electrophoresis on 1.5% (w/v) TAE agarose gel. DNA was purified using NucleoSpin® Gel and PCR Cleanup (TaKaRa Bio Inc., Japan), and its concentration and quality were assessed with a NanoDrop® system before DNA sequencing.

Results and discussion

Herein, we report a rare case of PMC in a young Japanese adult who presented with clinical symptoms resembling gonococcal keratoconjunctivitis. As shown in Fig. 1 (a), (b), these slit lamp photographs reveal a marked purulent discharge in the eyelids of right eye (a) and left eye (b). Additionally, slit lamp photographs show the bulbar and palpebral conjunctiva presenting with hyperemia and thickening in right eye (Fig. 1(c)) and left eye (Fig. 1(d)). Gram staining of the conjunctival swab identified the gram-negative diplococci, coffee bean appearance, as shown in Fig. 2. Furthermore, biochemical testing using the VITEK®2 NH card was performed, and the utilization capacity of glucose and maltose was confirmed to be positive, while that of sucrose and other sugars was confirmed to be negative.

Three colonies grew on blood agar, characterized by a grayish-white color, round shape, translucency, and glossy appearance. The colonies were centrifuged at 5,000 Xg at 4°C for five minutes, and the precipitate was placed on the pallet of the MALDI-TOF MS machine. As shown in Fig. 3a, the MALDI TOF raw mass spectra data was achieved using the autoflex speed™. We showed the obtained MALDI mass spectrum pattern (upper layer) and the standard pattern matching (lower layer) in Fig. 3b and c. The obtained the mass spectra pattern was compared and identified to the standard pattern matching with the Biotyper™ tool. As shown in Fig. 3, c, the score for *Neisseria meningitidis* is 2.165 by Biotyper™ database search (b), and that of *Neisseria gonorrhoeae* is 1.767 (c). Therfore, the pathogenic microorganism of this case was identified as *Neisseria meningitidis*, not *Neisseria gonorrhoeae.*

As shown in Fig. 4a, the PCR product was achieved approximately of 1600 bp in agarose gel electrophoresis. The 16S rRNA sequence for this PCR product compared with NCBI, and was showed the extremely high homology with a standard strain of Neisseria meningitidis, in Fig. 4b and 4c. The result of the direct DNA sequencing reconfirmed to support the identification with MALDI-TOF MS.

Our patient was 26 years old and had few systemic symptoms, with conjunctivitis and eye discharge as the main symptoms. PMC is extremely rare in adults. Barquet et al.[1] reviewed 84 cases of PMC globally from 1899 to 1988, and only 20 patients were adults (aged ＞18 years). Our literature search using PubMed yielded only a few additional case reports of adult PMC since 1990[5–11]. In Japan, there have been no reports of PMC in adults. In addition, our patient showed not only conjunctivitis but also stromal keratitis. We found several reported cases of keratitis, such as mild keratitis and perilimbal infiltrates, punctate epithelial

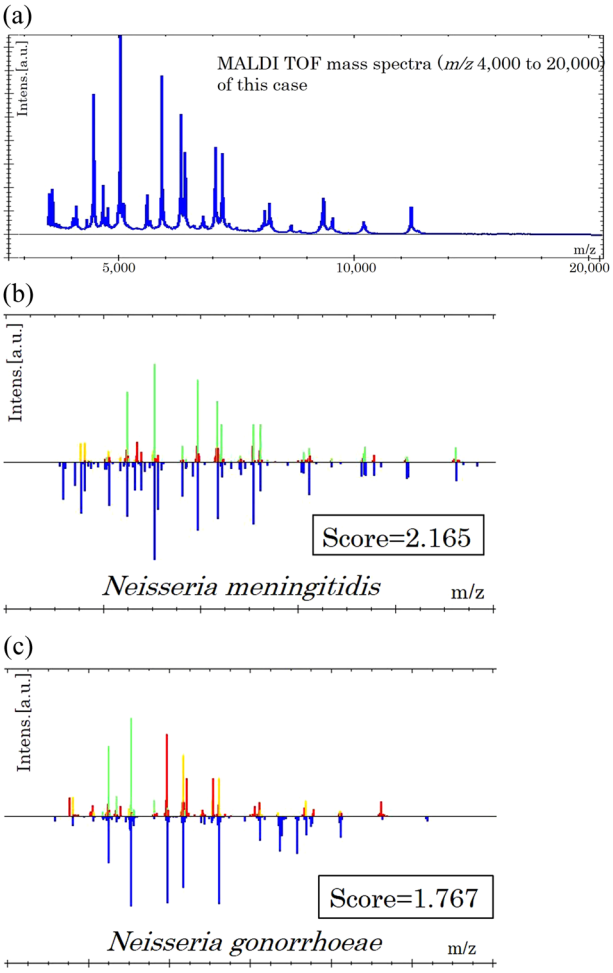

Fig. 3. MALDI-TOF mass spectra of this case and the score.

We analyze the standard pattern matching (a) and obtained MALDI mass spectrum pattern is compared to a database for identification.

The score for *Neisseria meningitidis* is 2.165 by Biotyper™ database search (b).

The score for Neisseria gonorrhoeae is 1.767 (c).

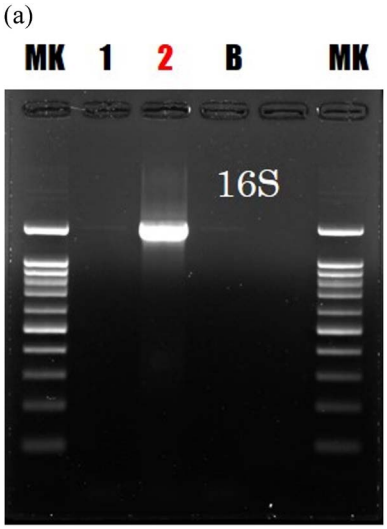

MK：marker, 1: other sample, 2: This case, B: dd-H2O

Fig. 4. The results of the image of the agarose electrophoresis and direct sequence of the PCR product of this case.

erosion of the cornea, subepithelial corneal infiltrates, peripheral stromal and limbal infiltrates, and corneal ulcers caused by *Neisseria meningitidis*[5, 7–11]. Unlike gonococcal conjunctival infections, no cases of corneal perforation have been observed in patients with PMC. PMC presents as an acute, purulent conjunctivitis and can mimic gonococcal conjunctivitis; however, differentiating between *Neisseria gonorrhoeae* and *Neisseria meningitidis* is important. PMC has the risk of corneal ulceration in 15.5% of cases, and after the onset of conjunctivitis, fatal systemic meningococcal infection (sepsis and/or meningitis) occurs in 10−29.9%, resulting in a high mortality rate of 13%[1, 12]. Moreover, Barquet et al.[1] reported that patients treated with only topical antibiotics develop systemic disease more frequently (approximately 32%) compared to those treated with both topical and systemic therapies (approximately 2%). Therefore, systemic therapy with adjunctive topical treatment is recommended to prevent invasive meningococcal infection in cases of hyperacute conjunctivitis caused by gram-negative diplococci[13–15].

In this case, gram-negative diplococci were confirmed, and gonococcal conjunctivitis was suspected; thus, systemic administration was promptly initiated. Fortunately, our patient did not develop a systemic meningococcal infection, and his ocular symptoms resolved. For the differentiation of between *Neisseria gonorrhoeae* and *Neisseria meningitidis*, both microbial and biochemical tests must be performed[16, 17]. The identification of *Neisseria* species. has always been considered a time-consuming task in routine laboratory work, and some publications have proposed tools to improve, accelerate, and simplify this process. MALDI-TOF MS is a new method for performing microbiology laboratory work that is capable of confirming the identity of several microorganisms known to be difficult to identify using conventional tests. Their method involves identifying a microorganism by searching a library for the ribosomal 16S protein. In our case, a gonococcal infection was suspected based on the clinical course, the patient's infection route episodes. However, using the MALDI-TOF MS method based on culture results, we were able to rapidly identify *Neisseria meningitidis* as the causative pathogen. As reported in reference[18], the MALDI-TOF MS

(b)

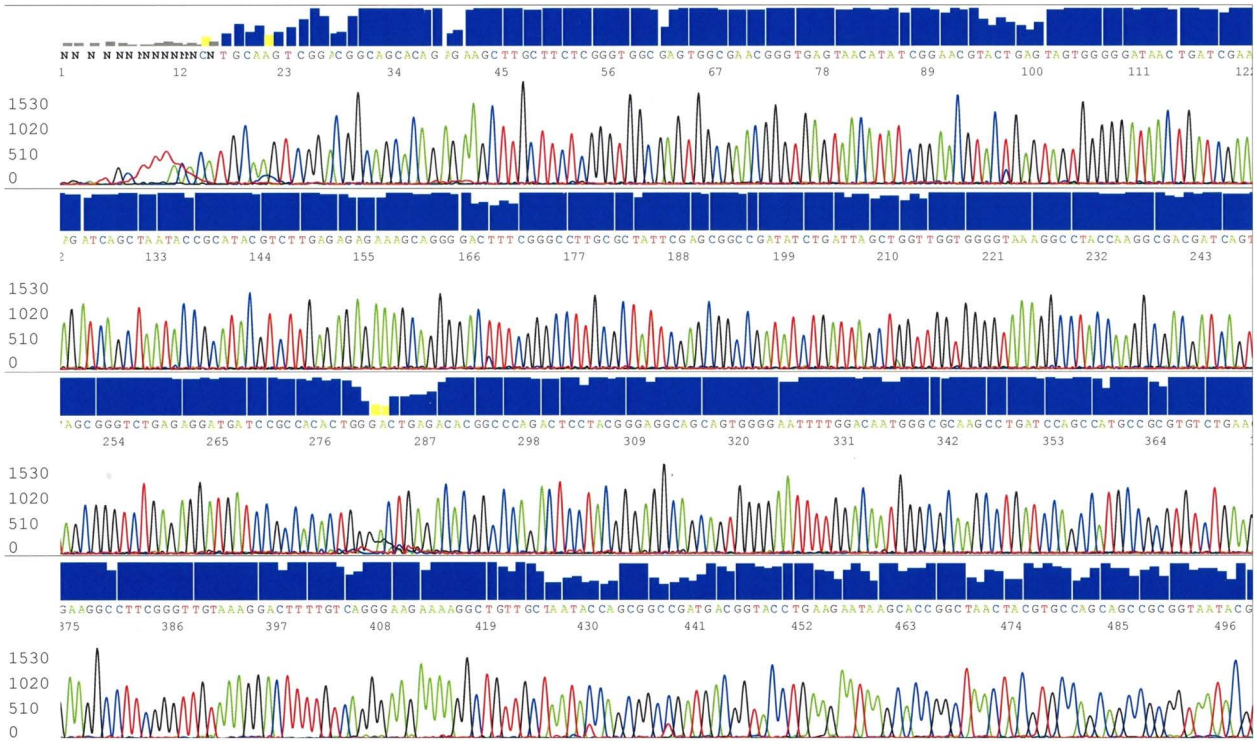

(c)

Neisseria meningitidis strain M1027 16S ribosomal RNA, partial sequence

Sequence ID: NR_104946.1 Length: 1415 Number of Matches: 1

Range 1: 1 to 638 GenBank Graphics Next Match Previou

Score	Expect	Identities	Gaps	Strand
1103 bits(597)	0.0	622/639(97%)	2/639(0%)	Plus/Plus

```
Query  12   GACGGCAGCACAGAGAAGCTTGCTTCTCGGGTGGCGAGTGGCGAACGGGTGAGTAACATA  71
Sbjct  1    GACGGCAGCACAGAGAAGCTTGCTTCTCGGGTGGCGAGTGGCGAACGGGTGAGTAACATA  60
Query  72   TCGGAACGTACTGAGTAGTGGGGGATAACTGATCGAAAGATCAGCTAATACCGCATACGT  131
Sbjct  61   TCGGAACGTACCGAGTAGTGGGGGATAACTGATCGAAAGATCAGCTAATACCGCATACGT  120
Query  132  CTTGAGAGAGAAAGCAGGGGACTTTCGGGCCTTGCGCTATTCGAGCGGCCGATATCTGAT  191
Sbjct  121  CTTGAGAGAGAAAGCAGGGGACCTTCGGGCCTTGCGCTATTCGAGCGGCCGATATCTGAT  180
Query  192  TAGCTGGTTGGTGGGGTAAAGGCCTACCAAGGCGACGATCAGTAGCGGGTCTGAGAGGAT  251
Sbjct  181  TAGCTAGTTGGTGGGGTAAAGGCCTACCAAGGCGACGATCAGTAGCGGGTCTGAGAGGAT  240
Query  252  GATCCGCCACACTGGGACTGAGACACGGCCCAGACTCCTACGGGAGGCAGCAGTGGGGAA  311
Sbjct  241  GATCCGCCACACTGGGACTGAGACACGGCCCAGACTCCTACGGGAGGCAGCAGTGGGGAA  300
Query  312  TTTTGGACAATGGGCGCAAGCCTGATCCAGCCATGCCGCGTGTCTGAAGAAGGCCTTCGG  371
Sbjct  301  TTTTGGACAATGGGCGCAAGCCTGATCCAGCCATGCCGCGTGTCTGAAGAAGGCCTTCGG  360
Query  372  GTTGTAAAGGACTTTTGTCAGGGAAGAAAAGGCTGTTGCTAATACCAGCGGCCGATGACG  431
Sbjct  361  GTTGTAAAGGACTTTTGTCAGGGAAGAAAAGGCTGTTGCTAATATCAGCGGCTGATGACG  420
Query  432  GTACCTGAAGAATAAGCACCGGCTAACTACGTGCCAGCAGCCGCGGTAATACGTAGGGTG  491
Sbjct  421  GTACCTGAAGAATAAGCACCGGCTAACTACGTGCCAGCAGCCGCGGTAATACGTAGGGTG  480
Query  492  CGAGCGTTAATCGGAATTACTGGGCGTAAAGCGGGCGCAGACGGTTACTTAAGCNGGATG  551
```

Fig. 4. Continued.

The agarose gel electrophoresis patterns of the PCR products of this case (a).
The result of the direct sequence of the r16S PCR product in this case (b).
The identification of Neisseria meningitidis by Database search (GeneBankTM) (c).

method is a powerful tool for more rapidly identifying pathogenic microorganisms compared to the 16S rRNA sequencing method. From the perspective of a mass spectrometry expert, microbial identification using MS is essentially a pattern recognition of the r16S protein, and does not involve indentifying or comparing individual proteins, Therefore, it is believed that the method may be usable even with crude samples. We believe that this allowed for the appropriate isolation of patients and prevention of infection. Fatalities after acquiring PMC from close contacts have been reported[1, 9, 12]. Therefore, individuals who were in close contact with patients should be administed with

prophylactic antibiotics (such as ciprofloxacin), and intervention by infection control experts is required to prevent disease outbreaks. The risk of infection during a close slit-lamp examination is unknown; however, in this case, upon the advice of the hospital's infection control department, the patient was isolated in a private room for one week, and close contacts were administered ciprofloxacin tablets (500 mg).

In summary, we report a rare case of PMC in a young adult Japanese patient. Prompt and precise diagnosis from clinical eye findings and bacterial identification tests by ophthalmologists is important to initiate appropriate systemic antimicrobial therapy to prevent systemic disease and disease outbreaks. The MALDI-TOF MS analysis was a very useful for the rapid identification of *Neisseria meningitidis*.

Statement of ethics

This study complied with the guidelines for human studies and was conducted ethically, following the World Medical Association Declaration of Helsinki. Written informed consent was obtained from the patient for publication of this case report and any accompanying images. The Ethics Committee of our institute, Osaka Medical and Pharmaceutical University does not require an ethical approval for this study in accordance with local guidelines. The authors have no ethical conflicts to disclose.

Conflict of interest

The authors have no conflicts of interest to declare.

Funding sources

This study was not supported by any sponsor or funder.

Acknowledgements

I would like to express my appreciation for the test results and advice provided by the Microbiology Laboratory of the Central Testing Department at Osaka Medical and Pharmaceutical University Hospital.

References

1) Barquet N, Gasser I, Domingo P, Moraga FA, Macaya A, et al: Primary meningococcal conjunctivitis: report of 21 patients and review. *Rev Infect Dis* 12: 838−847, 1990.
2) Anderson J, Lind I: Characterization of Neisseria meningitidis isolates and clinical features of meningococcal conjunctivitis in ten patients. *Eur J Clin Microbiol Infect Dis* 13: 388−393, 1994.
3) Wieser A, Schneider L, Jung J, Schubert S: MALDI-TOF MS in microbiological diagnostics-identification of microorganisms and beyond (mini review). *Appl Microbiol Biotechnol* 93: 965−974, 2012.
4) Seng P, Rolain JM, Fournier PE, LaScola B, Drancourt M, et al: MALDI-TOF-mass spectrometry applications in clinical microbiology. *Future Microbiol* 5: 1733−1754, 2010.
5) Andreoli CM, Wiley HE, Durand ML, Watkins LM: Primary meningococcal conjunctivitis in an adult. *Cornea* 23: 738−739, 2004.
6) Irani F, Ruddell T: Meningococcal conjunctivitis. *Aust N Z J Ophthalmol* 25: 167−168, 1997.
7) Stansfield RE, Masterton RG, Dale BA, Fallon RJ: Primary meningococcal conjunctivitis and the need for prophylaxis in close contacts. *J Infect* 29: 211−214, 1994.
8) Garcia-Lechuz JM, Alcala L, Gijon P, San Juan R, Bouza E: Primary meningococcal conjunctivitis in a human immunodeficiency virus-infected adult. *Clin Infect Dis* 27: 1556−1557, 1998.
9) Dryden AW, Rana M, Pandey P: Primary meningococcal conjunctivitis: an unusual case of transmission by saliva. *Digit J Ophthalmol* 22: 25−27, 2016.
10) Aranzasti C, Aguirreburualde R, Martinez R, Durán de la Colina JA, Gaztelurrutia L: Primary meningococcal keratoconjunctivitis in an extended contact lenses wearer. *Br J Ophthalmol* 78: 731, 1994.
11) Elias JA, Pandit RT: Primary Neisseria meningitidis Keratitis. *Cornea* 28: 714−715, 2009.
12) Parikh SR, Campbell H, Mandal S, Ramsay ME, Ladhani SN: Primary meningococcal conjunctivitis: Summary of evidence for the clinical and public health management of cases and close contacts. *J Infect* 79: 490−494, 2019.
13) Orden B, Martinez R, Millon R, Belloso M, Perez N: Primary meningococcal conjunctivitis. *Clin Microbiol Infect* 9: 1245−1247, 2003.
14) Andreoli CM, Wiley HE, Durand ML, Watkins LM: Primary meningococcal conjunctivitis in an adult. *Cornea* 23: 738−739, 2004.
15) Kanda P, Ioannidis S, Sim W, Weston B, Koaik M: Primary meningococcal conjunctivitis in an adult patient. *IDCases* 32: e01749, 2023.
16) Buchanan R, Ball D, Dolphin H, Dave J: Matrix-assisted laser desorption-ionization time-of-flight mass spectrometry for the identification of Neisseria gonorrhoeae. *Clin*

Microbiol Infect 22: 815−815, 2016.

17) Ilina EN, Borovskaya AD, Malakhova MM, Vereshchagin VA, Kubanova AA, et al: Direct bacterial profiling by matrix-assisted laser desorption ionization time-of-flight mass spectrometry for identification of pathogenic neisseria. *J Mol Diagn* 11: 75−86, 2009.

18) Mellmann A, Cloud J, Maier T, Keckevoet U, Ramminger I, et al: Evaluation of matrix-assisted laser desorption ionization-time-of-flight mass spectrometry in comparison to 16S rRNA gene sequencing for species identification of nonfermenting bacteria. *J Clin Microbiol* 46: 1946−1954, 2008.

Medical Mass Spectrometry Vol. 9 No. 1, 2025

Publication Date: June 25, 2025
Publisher: Japanese Society for Biomedical Mass Spectrometry
6 Nikko-cho, Ichinomiya, Aichi 491−0938, Japan
Shubun University
Instructions for Authors: http://www.jsbms.jp/english/doc/inst_en.pdf
Printer: International Academic Publishing Co., Ltd.